REVIEWS

Journal of Semiconductors
(2023) 44, 081701
doi: 10.1088/1674-4926/44/8/081701

State-of-the-art advances in vacancy defect engineering of graphitic carbon nitride for solar water splitting

Jie Li[1, 2, ‡], Kaige Huang[3, 4, 5, ‡], Yanbin Huang[2, †], Yumin Ye[6], Marcin Ziółek[7], Zhijie Wang[3, 4, 5, †], Shizhong Yue[3, 4, 5, †], Mengmeng Ma[3, 4, 5], Jun Liu[8], Kong Liu[3, 4, 5], Shengchun Qu[3, 4, 5], Zhi Zhao[2], Yanjun Zhang[2], and Zhanguo Wang[3, 4, 5]

[1]College of Mechanical and Electrical Engineering, Handan University, Handan 056005, China

[2]Hebei International Joint Research Center for Computational Optical Imaging and Intelligent Sensing, Hebei International Joint Research Center for Computational Optical Imaging and Intelligent Sensing, School of Mathematics and Physics Science and Engineering, Hebei University of Engineering, Handan 056038, China

[3]Key Laboratory of Semiconductor Materials Science, Institute of Semiconductors, Chinese Academy of Sciences, Beijing 100083, China

[4]Beijing Key Laboratory of Low Dimensional Semiconductor Materials and Devices, Beijing 100083, China

[5]Center of Materials Science and Optoelectronics Engineering, University of Chinese Academy of Sciences, Beijing 100049, China

[6]Department of Materials Science and Engineering, Faculty of Materials Science and Chemical Engineering, Ningbo University, Ningbo 315211, China

[7]Faculty of Physics, Adam Mickiewicz University Poznan, 61-614 Poznan, Poland

[8]Guangdong-Hong Kong Joint Laboratory for Water Security, Engineering Research Center of Ministry of Education on Groundwater Pollution Control and Remediation, Center for Water Research, Advanced Institute of Natural Sciences, Beijing Normal University at Zhuhai, Zhuhai 519087, China

Abstract: Developing low-cost, efficient, and stable photocatalysts is one of the most promising methods for large-scale solar water splitting. As a metal-free semiconductor material with suitable band gap, graphitic carbon nitride (g-C_3N_4) has attracted attention in the field of photocatalysis, which is mainly attributed to its fascinating physicochemical and photoelectronic properties. However, several inherent limitations and shortcomings—involving high recombination rate of photocarriers, insufficient reaction kinetics, and optical absorption—impede the practical applicability of g-C_3N_4. As an effective strategy, vacancy defect engineering has been widely used for breaking through the current limitations, considering its ability to optimize the electronic structure and surface morphology of g-C_3N_4 to obtain the desired photocatalytic activity. This review summarizes the recent progress of vacancy defect engineered g-C_3N_4 for solar water splitting. The fundamentals of solar water splitting with g-C_3N_4 are discussed first. We then focus on the fabrication strategies and effect of vacancy generated in g-C_3N_4. The advances of vacancy-modified g-C_3N_4 photocatalysts toward solar water splitting are discussed next. Finally, the current challenges and future opportunities of vacancy-modified g-C_3N_4 are summarized. This review aims to provide a theoretical basis and guidance for future research on the design and development of highly efficient defective g-C_3N_4.

Key words: g-C_3N_4; vacancy defect; water splitting; photocatalyst; charge carrier

Citation: J Li, K G Huang, Y B Huang, Y M Ye, M Ziółek, Z J Wang, S Z Yue, M M Ma, J Liu, K Liu, S C Qu, Z Zhao, Y J Zhang, and Z G Wang, State-of-the-art advances in vacancy defect engineering of graphitic carbon nitride for solar water splitting[J]. *J. Semicond.*, 2023, 44(8), 081701. https://doi.org/10.1088/1674-4926/44/8/081701

1. Introduction

With the world's over-dependence on energy and the increasing impact of fossil energy on the global climate and environment, there has never been greater urgency to exploit cleaner and renewable energy supplies[1]. Hydrogen is a clean energy with high energy density and is carbon free, which makes it a promising alternative to traditional fossil fuels and has attracted much attention. However, nearly 85% of global hydrogen production is obtained by gas reforming, which relies on fossil fuels and releases approximately 500 metric tons of carbon dioxide (CO_2) per year as a byproduct. Thus, producing hydrogen via photocatalytic water splitting, so-called artificial photosynthesis, has emerged as one of the most promising approaches to capturing and converting solar energy into clean energy[2]. Since H_2 production by means of water splitting using semiconductor titanium dioxide (TiO_2) as a photocatalyst was discovered by Fujishima and Honda, numerous semiconductors have been developed for solar water splitting[3]. However, most metal-oxide semiconductors can only respond to a small part of the solar spectrum due to their wide bandgaps. Although metal sulfides, metal phosphides, and metal nitrides photocatalysts have a narrow bandgap, their instability and deleterious properties severely limit their wide use as photocatalysts[4]. In addition, none of them demonstrate the desired performance for solar water

Jie Li and Kaige Huang contributed equally to this work and should be considered as co-first authors.

Correspondence to: Y B Huang, huangyb@hebeu.edu.cn; Z J Wang, wangzj@semi.ac.cn; S Z Yue, yueshizhong@semi.ac.cn

Received 8 FEBRUARY 2023; Revised 1 MARCH 2023.

splitting. As a result, the commercial application of solar water splitting is hampered by the low efficiency of solar to hydrogen (STH) conversion[5, 6]. Thus far, developing semiconductor photocatalysts that are highly efficient, abundant, and stable for practical application is still a challenge and has received extensive attention.

Recently, two-dimensional (2D) materials have been widely used in solar energy conversion, due to their excellent physicochemical and optoelectronic properties[7, 8]. Among the various 2D semiconductor materials, g-C_3N_4 has attracted extensive attention because of its advantageous characteristics, such as appropriate and tunable band structure with visible-light response, good chemical and thermal stability, non-toxicity, it is composed of earth-abundant elements, and is easy to process. Therefore, g-C_3N_4-based materials are believed to be among of the most promising candidates for environmental and energy-concerned photocatalytic reactions[9]. Despite these mentioned advantages, pristine g-C_3N_4 still suffers from several obstacles and shortcomings, which are caused by low crystallinity and high degree of disorders and defects, such as poor visible-light responsiveness at longer wavelengths, relatively small solvent-accessible surface area, low charge migration rate, and high recombination of photogenerated charge carriers[10].

To surmount these shortcomings, many efforts have been made to optimize the photocatalytic efficiency and performance of g-C_3N_4. In addition, many strategies have been reported to construct high crystallinity, doped, heterostructured and functionalized g-C_3N_4 to achieve target-specific applications[11–13]. In most cases, defect engineering is recognized as an effective method to break through the existing limitations, which can achieve the desired physicochemical properties by tuning the electrical structure and surface morphology[14, 15]. Usually, defects in crystals can be divided into different categories according to their dimensions, such as point defects (vacancies, replacement, interstitial defects, etc.), line defects (steps, dislocations, etc.), planar defects (stacking fault, grain boundary, etc.) and bulk defects (impurities, voids, etc.). In particular, the introduction of point defects, such as vacancy or doping, into the structural unit of g-C_3N_4 has been extensively studied to improve the photocatalytic activity of g-C_3N_4. However, the doping of foreign atoms is usually accompanied by some negative consequences. For example, it is difficult to characterize the spatial distribution and ensure a uniform distribution of dopants, which is crucial for the effective regulation of the electronic structure of g-C_3N_4[16]. Thus, it is intriguing to investigate the positive influence of point defect modification (specifically vacancy generation) in g-C_3N_4 for solar water splitting, which has been extensively studied in recent years. For example, the generated carbon (C) or nitrogen (N) vacancies can act as additional reactive sites and enlarge the surface area, regulate the electronic band structure, serve as trap states and increase electrical conductivity, and enhance the transfer and separation efficiency of photogenerated charge carriers[16–18]. In addition, the generated vacancy defects may induce abundant localized electrons, which is helpful for the adsorption and activation of gas molecules[19]. Therefore, a comprehensive study of vacancy defects is crucial to understand defect engineering and explore high-efficiency photocatalysts.

In this context, there have been several brilliant reviews

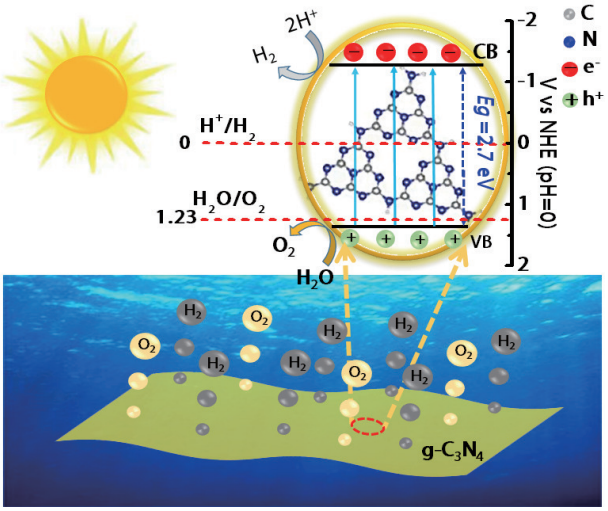

Fig. 1. (Color online) Schematic illustration of the fundamental mechanism of solar water splitting with g-C_3N_4.

that have concentrated on introducing vacancies to engineer the photocatalytic performance of g-C_3N_4[14–16, 20]. However, to the best of our knowledge, previous reviews have paid less emphasis on the vacancy defect engineering of g-C_3N_4 photocatalysts for solar water splitting. Thus, a timely and updated review of vacancy defect engineering of g-C_3N_4 is necessary to advance the rapidly progressing pace of this subject. Herein, we aim to provide a comprehensive review of the recent advances in vacancy defect engineered g-C_3N_4 photocatalysts that are employed in solar water splitting. We will first briefly introduce the vacancy defect engineering of g-C_3N_4 in photocatalysis and the fundamental mechanism of photocatalytic water splitting with g-C_3N_4. We will then present the strategies for the fabrication of vacancy defect g-C_3N_4, such as thermal, chemical, and other treatment strategies. We will then focus on the effect of vacancy defect on the band structure, the separation and transfer performance of charge carriers, and surface reaction kinetics of g-C_3N_4. The role of vacancy defect g-C_3N_4 in solar water splitting will then be summarized. Finally, this review will discuss some novel insights on the crucial challenges, future opportunities, and inspiring perspectives in the vacancy defect engineering of g-C_3N_4.

2. Fundamental of photocatalytic water splitting by g-C_3N_4

Generally, solar water splitting can be divided into three crucial steps: (i) light absorption by a photocatalyst, which can excite the electrons from the lower valence band (VB) to the conduction band (CB), resulting in the formation of holes in VB; (ii) separation and migration of photogenerated charge carriers to the surface of photocatalyst; and (iii) stimulation of charge carriers participating in a redox reaction to split water into H_2 and O_2. Moreover, water splitting is a four-electron and nonspontaneous process that requires a Gibbs free energy of 237 kJ/mol to overcome the energy barrier of 1.23 eV for the facile functioning of solar water splitting reaction[21, 22]. Therefore, a photocatalyst with appropriate band structure is indispensable for an overall photocatalytic water splitting.

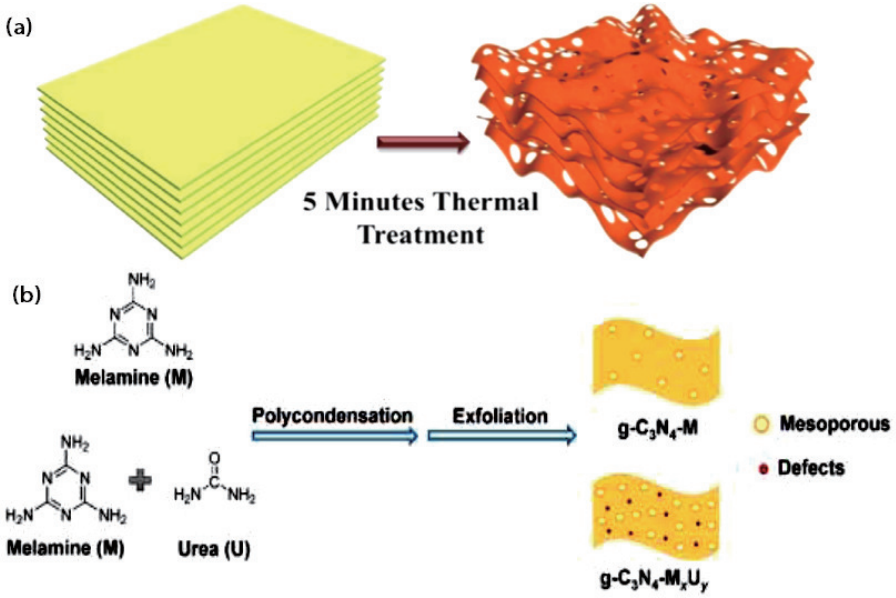

Fig. 2. (Color online) Schematic illustration of the preparation of vacancy-modified g-C_3N_4 by thermal treatment method. (a) Direct calcination of bulk g-C_3N_4 (Copyright 2018, Elsevier)[27]. (b) Using melamine (M) or a mixture of M and urea (U) as the precursors (Copyright 2018, Elsevier)[17].

Generally, the potential of the lowest unoccupied molecular orbital (LUMO) or the bottom edge of CB for a semiconductor photocatalyst has to be more negative than the redox potential of H^+/H_2 (0 V vs NHE at pH 0), while the redox potential of the highest occupied molecular orbital (HOMO) or VB has to be more positive than the redox potential of O_2/H_2O (1.23 V vs NHE at pH 0). However, due to the high over-potentials during the process of the water splitting reaction, a bandgap of 1.23 eV is insufficient for driving the redox reaction, and the bandgap of the participating photocatalyst must be in the visible-light range of 1.6–2.4 eV[23, 24]. As illustrated in Fig. 1, the bandgap of g-C_3N_4 is about 2.7 eV. The bottom edge of CB lies at about −1.3 V versus NHE and is much more negative than the potentials of H_2 evolution, while the top edge of VB locates at about 1.4 V and is sufficient for oxygen evolution[25]. In practice, by considering thermodynamic losses and over-potentials, the bandgap of g-C_3N_4 usually varies in a range of 2.0–3.1 eV, which is sufficient for driving the redox reaction of solar water splitting and implies good visible-light absorption performance. However, the redox reaction potentials of water splitting are stringent, which requires the band edges of the photocatalyst to strictly meet the potentials of reduction or oxidation. Therefore, defect engineering is necessary, which can regulate the band structure of g-C_3N_4 within a suitable range, resulting in an optimized balance between redox reaction driving force, light absorption, charge carriers transfer, and separation efficiency, which improves the photocatalytic efficiency of solar water splitting.

3. Strategy for the fabrication of vacancy defect g-C_3N_4

Generally, there are two main ways to introduce defects into g-C_3N_4. The first is the top-down method that introduces defects into pre-synthesized g-C_3N_4, which is a widely used strategy and can easily introduce vacancies into the surface or body of g-C_3N_4. The generation of defects in prepared g-C_3N_4 is independent of the growth kinetics of the crystal, which is widely employed for the introduction of defects (e.g., the generation of voids, vacancy, and disorder). The key of this method is to select appropriate additives for defect generation. The second is the bottom-up approach that introduces defects during the formation process of g-C_3N_4, which is another important strategy for the generation of vacancy defects and largely relies on the growth kinetics of semiconductors[26]. To date, a number of g-C_3N_4 containing vacancy defects have been synthesized via these two strategies. In this section, the frequently utilized methods are summarized, including thermal treatment, chemical treatment, and some other treatment methods.

3.1. Thermal treatment

Thermal treatment is a widely utilized strategy to introduce vacancies, which can be employed to create vacancies in g-C_3N_4 by direct calcination or selecting a suitable etching agent to assist in removing determined atoms. Directly calcining g-C_3N_4 at high temperature without etchant is a simple method that can be utilized to create vacancy defects in g-C_3N_4, which is mainly attributed to the cleavage of bonds. In addition, the escape of atoms from the lattice could be accelerated at high temperature. Moreover, the thermal treatment can break some bonds on each sheet of bulk g-C_3N_4 and lead to the formation of vacancies. As illustrated in Fig. 2(a), Niu *et al*. synthesized porous structured g-C_3N_4 materials with a large number of defects via facile thermal treatment for 5 min in air without additional reactants. The characterization analyses indicated that N vacancies and cyano groups were introduced into the framework of g-C_3N_4. As a result, the light absorption edge and hydrogen evolution rate of the optimized g-C_3N_4 were remarkably enhanced during the solar water splitting process[27]. Similarly, direct thermal treatment of the g-C_3N_4 precursor at high temperature is another simple method for preparing vacancy defect g-C_3N_4. As shown in Fig. 2(b), Ruan *et al*. obtained N-deficient g-C_3N_4 by a novel thermal treatment strategy that used a mixture of melamine and urea as the precursors[17]. Niu *et al*. synthesized N-deficient g-C_3N_4 by directly heating dicyandiamide in static air at 600 °C. The results showed that N vacancies were facilely intro-

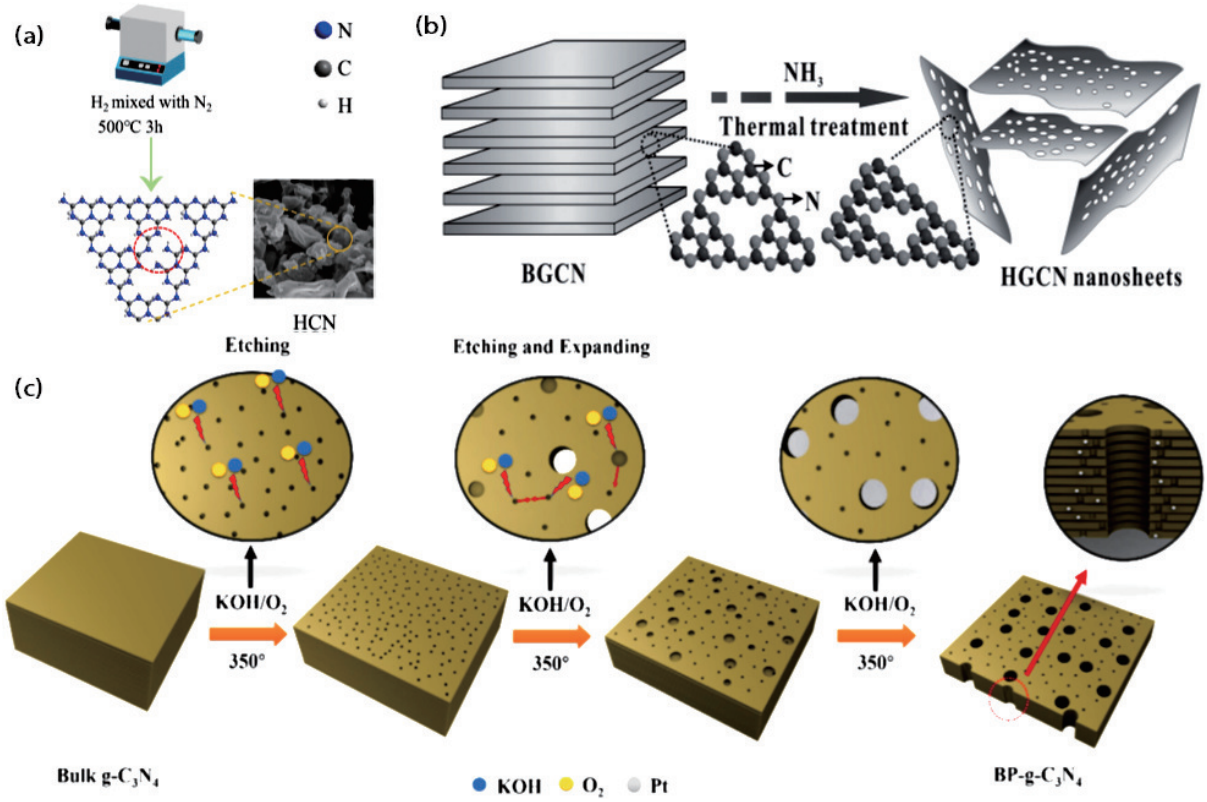

Fig. 3. (Color online) Schematic illustration of the preparation of vacancy-modified g-C_3N_4 by thermal treatment method with suitable etching agent. The vacancy-modified g-C_3N_4 was prepared using (a) H_2 mixed with N_2 (Copyright 2022, Elsevier)[31], (b) NH_3 (Copyright 2015, Wiley)[32], and (c) KOH as etching agents (Copyright 2018, Elsevier)[34], respectively.

duced in the framework of g-C_3N_4 after the thermal treatment[28]. Similarly, Han *et al*. successfully introduced N vacancies and disordered structure into g-C_3N_4 by directly calcining the rational size reduced urea crystals obtained from an antisolvent growth method[29].

Vacancy defect g-C_3N_4 can also be prepared by a thermal treatment method with a suitable etching agent, which is helpful to remove specific atoms of g-C_3N_4 and facilitate precise control of the type of introduced defects. The three commonly used etching agents are gas, acid, and alkali. Generally, the gas etching method can not only realize the introduction of vacancy defects but also facilitate the exfoliation of the stacked layers and obtain nanosheets with many in-plane holes. As reported by Niu *et al*., g-C_3N_4 with N vacancies was prepared by calcination of bulk g-C_3N_4 under H_2 atmosphere. It was discovered that the H_2 treatment could reduce the lattice N into NH_3 and introduce N vacancies[30]. As shown in Fig. 3(a), Li *et al*. reported that g-C_3N_4 materials with ample C vacancies could be synthesized by calcinating g-C_3N_4 in H_2 and N_2 gas mixture. It was found that C vacancies generated in the N-(C_3) bond lead to the reduction of electron density around N, thus narrowing the bandgap of g-C_3N_4 and improving corresponding light response capability[31]. Additionally, Liang *et al*. demonstrated that C vacancies can be introduced to the g-C_3N_4 through the treatment of bulk g-C_3N_4 in NH_3 atmosphere (Fig. 3(b)). It was found that the NH_3 etching not only facilitated the exfoliation of bulk g-C_3N_4 but also introduced C vacancy by removing g-C_3N_4 species[32].

Acid etching and alkali etching can also be used to generate vacancy defects, which can control the number of defects introduced into g-C_3N_4 in comparison with gas etching. For instance, Wang *et al*. developed an atom-thin g-C_3N_4 sheets with N vacancy via a fluorination followed by thermal defluorination strategy. The experimental characterization and theoretical calculations revealed that this method could introduce cyano groups into the structure of g-C_3N_4 and the accompanied N vacancies at the edges, which both narrowed the bandgap and changed the charge distribution[33]. As demonstrated in Fig. 3(c), Hu *et al*. presented a novel and cost-effective KOH activation and thermal oxidation strategy for preparing hierarchically bimodal porous g-C_3N_4 nanosheets. It was found that the reaction between KOH and g-C_3N_4 could consume g-C_3N_4 and lead to the formation of pores, introducing vacancy defects into g-C_3N_4[34]. Meanwhile, different types of vacancies may play different roles, which can directly affect the adjustment of g-C_3N_4. To investigate the diverse properties of different types of N vacancies, Xie *et al*. synthesized a g-C_3N_4 with two types of N vacancies via a one-pot KOH-assisted calcination treatment method. Their characterization indicated that the introduced NH_x and N_{2C} vacancies were mainly attributed to the KOH etching treatment, and the NH_x and N_{2C} vacancy played the role of photoexcited charges separation and O_2 activation in the two-electron process, respectively. This work provides a novel strategy for designing high-efficiency g-C_3N_4 with different types of N vacancies[35]. Consequently, thermal treatment is a widely utilized and effective strategy for introducing vacancy in g-C_3N_4.

3.2. Chemical treatment

Chemical treatment is an effective approach to generating vacancy defects in g-C_3N_4 by using chemicals such as molten alkali, molten salts, and organic acids. A suitable chemical environment is important for introducing and regulating

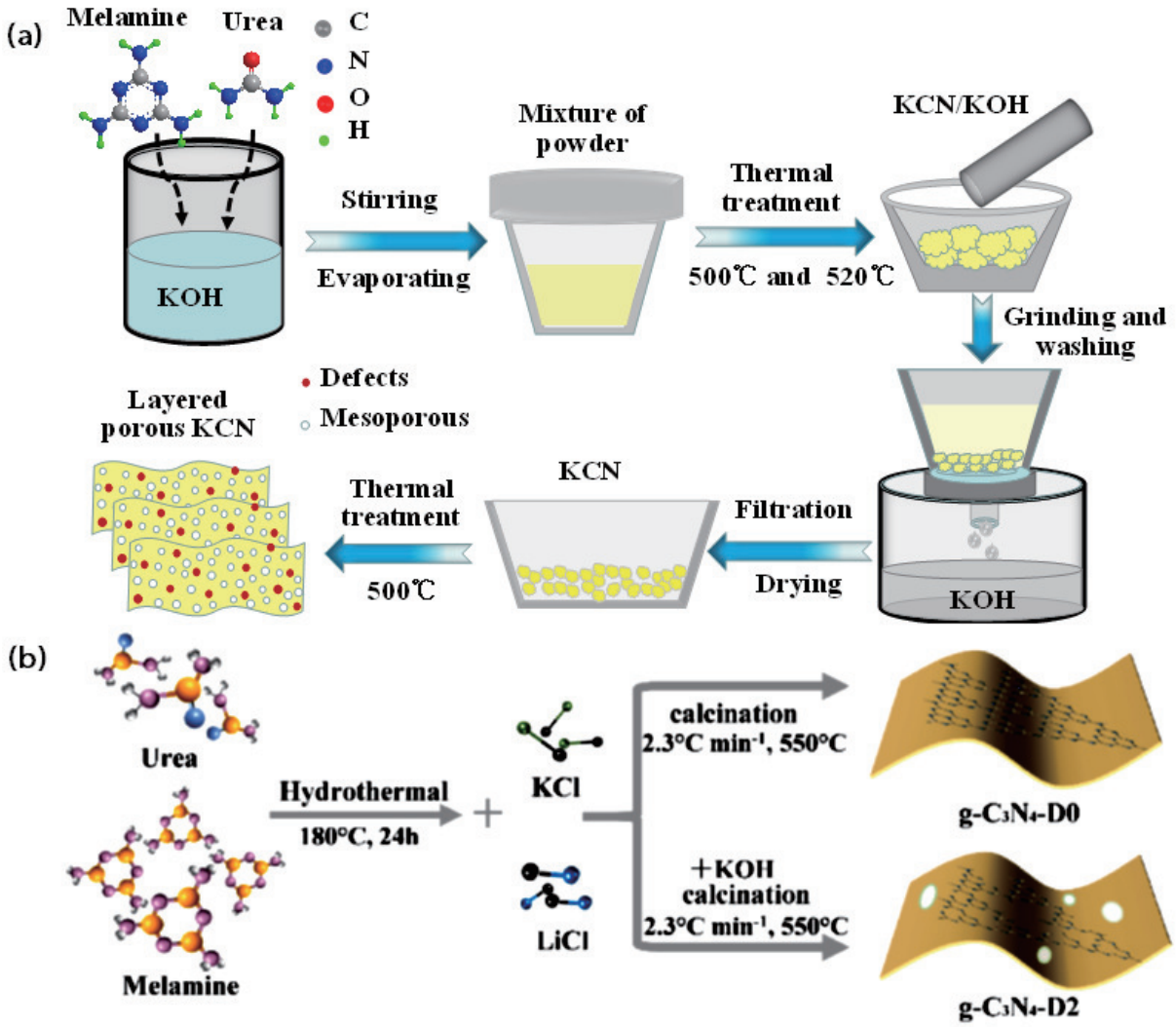

Fig. 4. (Color online) Schematic illustration of the preparation of vacancy-modified g-C_3N_4 by strong alkali treatment of prepared g-C_3N_4 or its precursors. The vacancy-modified g-C_3N_4 was prepared by (a) the facile urea- and KOH-assisted thermal polymerization strategy (Copyright 2020, American Chemical Society)[18], (b) the alkali-molten salt-assisted method (Copyright 2023, Elsevier), respectively[37].

vacancy in g-C_3N_4, which can effectively regulate the photocatalytic performance of g-C_3N_4. Strong alkali treatment of g-C_3N_4 or its precursors are commonly opted approaches to preparing vacancy defect g-C_3N_4. For instance, the treatment of g-C_3N_4 precursors with KOH leads to the formation of pores on the surface of g-C_3N_4 during the thermal oxidation and polymerization process, which is beneficial for the introduction of vacancy defects in g-C_3N_4. Inspired by this, Yu *et al*. developed a novel one-step KOH-assisted method to synthesize N defective g-C_3N_4. In this study, the cyano group and N vacancy were successfully introduced into g-C_3N_4 through adding an alkali compound such as KOH during the thermal polymerization of urea or other nitrogen-rich precursors, which resulted in redshifted absorption edge. In addition, the amount of N defects could be facilely regulated by the KOH: urea ratio. Similar results were achieved using other alkali compounds (e.g., NaOH and $Ba(OH)_2$), which indicated the versatility of this strategy[36]. In another study, as shown in Fig. 4(a), our group developed facile and effective urea (U)- and KOH-assisted strategy to regulate the property of g-C_3N_4, wherein the mesopores, cyano groups, and N vacancies could be simultaneously introduced into g-C_3N_4 during the thermal polymerization of the alkali containing precursor, and the roles of thickness, pores, and defects could be intentionally modulated and optimized by changing the mass ratio of urea, KOH, and melamine. Importantly, the synergistic modulation of thickness pores and N defects can remarkably increase the specific area, improve the light-harvesting capability and photogenerated charge carries separation efficiency, and strengthen the mass transfer in g-C_3N_4[18]. Recently, Shao *et al*. also reported a simple alkali-molten salt-assisted method to fabricate N-deficient crystalline g-C_3N_4, wherein N-vacancy crystalline g-C_3N_4 nanosheets with tunable band structures were successfully prepared during the alkali-molten salt-assisted hydrothermal polymerization process (Fig. 4(b))[37]. These strategies with tunable properties will open up further opportunities to modify g-C_3N_4 toward advanced applications.

Salt treatment of g-C_3N_4 or its precursors is another widely utilized strategy for developing vacancy-modified g-C_3N_4. On the one hand, salts with high reluctivity generate active substances during the thermal treatment process, which can destroy the molecular configuration of g-C_3N_4 and introduce vacancy defects. $NaBH_4$ is a classic reducing agent used to prepare defective g-C_3N_4. For instance, Qin *et al*. presented a logical method for integrating N defect engineering

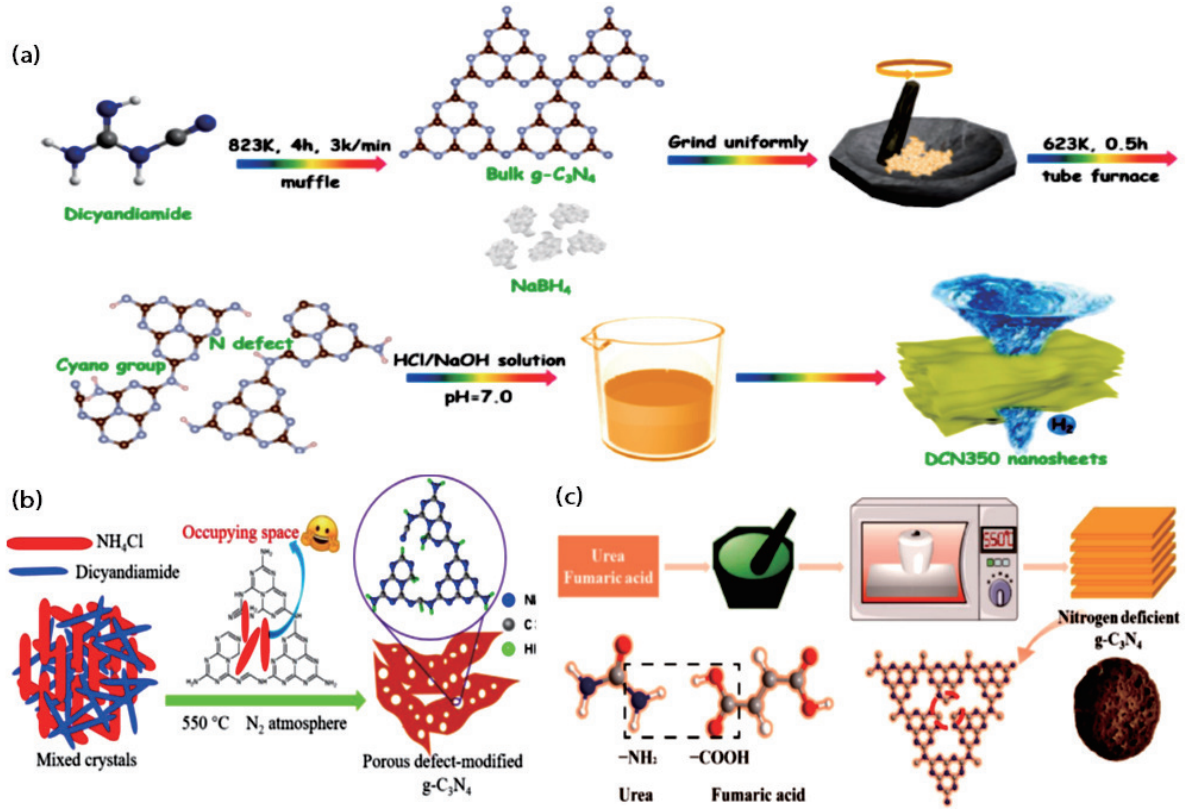

Fig. 5. (Color online) Schematic illustration of the preparation of vacancy-modified g-C_3N_4 by chemical treatment strategy. The vacancy-modified g-C_3N_4 were prepared by (a) the calcination of g-C_3N_4 and $NaBH_4$ strategy (Copyright 2019, Wiley)[39], (b) thermally polymerizing the mixture of dicyandiamide and NH_4Cl method (Copyright 2020, Elsevier)[40], and (c) thermal polymerization of the mixture of fumaric acid and urea (Copyright 2021, American Chemical Society), respectively[43].

and π-conjugation structure into g-C_3N_4, wherein the low-temperature calcination of g-C_3N_4 and $NaBH_4$ not only led to the preferment loss of lattice N and the synchronous breakdown of the s-triazine heterocycle but also generated new –C≡N group[38]. In another study, Zhao *et al*. successfully introduced boron dopants and N defects into g-C_3N_4 through calcining the mixture of g-C_3N_4 and $NaBH_4$ in a nitrogen atmosphere. As shown in Fig. 5(a), during the thermal polymerization process, hydrogen and boron released from $NaBH_4$ would react with the C and C atoms in the framework of g-C_3N_4 and produce ammonia and alkanes gases. Boron-doped and nitrogen-deficient g-C_3N_4 was then finally synthesized, wherein amino group (–NH_2) was decomposed and cyano was introduced by breaking C–N–C bonds, along with the doping of boron atoms at carbon sites[39]. Furthermore, some ammonium salts (such as NH_4Cl, NH_4I, $(NH_4)_2S_2O_8$) play an important role in occupying space to limit long-distance polymerization, which may lead to the introduction of defects into the g-C_3N_4 during the thermal polymerization process[40–42]. For example, Zhang *et al*. developed a novel one-step strategy to synthesize porous g-C_3N_4 with vacancy defects by thermally polymerizing the freeze-dried mixture of dicyandiamide and NH_4Cl under the nitrogen atmosphere (Fig. 5(b)). The experimental characterizations confirmed that dicyandiamide would polymerize into melamine at 234 °C, while NH_4Cl would decompose at 337 °C, the undecomposed NH_4Cl would play a role in separating some dicyandiamide crystal grains and dicyandiamide derived intermediates in space and inhibiting the formation of integrated tri-s-triazine structure. As a result, the cyano group and N vacancy were introduced into the prepared g-C_3N_4[40]. Similarly, Jiang *et al*. proposed a simple co-pyrolysis of dicyandiamide and ammonium persulfate ($(NH_4)_2S_2O_8$) approach to introducing the porous structure, N defects, and O dopants into the framework of g-C_3N_4 simultaneously. Due to the difference between the thermal polymerization temperature of dicyandiamide and the decomposition temperature of $(NH_4)_2S_2O_8$, the gases generated from the decomposed $(NH_4)_2S_2O_8$ could suppress the formation of complete tri-s-triazine structure at 550 °C, which led to the generation of N in the skeleton of g-C_3N_4[42].

Acid-assisted thermal treatment of g-C_3N_4 or its precursors is also widely used to fabricate vacancy-modified g-C_3N_4. For instance, Yu *et al*. proposed a simple and green approach to constructing N defective g-C_3N_4. As shown in Fig. 5(c), g-C_3N_4 with N vacancies was fabricated by one-pot thermal polymerization of the mixtures of fumaric acid and urea. The study further revealed that the carboxyl group (–COOH) of fumaric acid reacted with –NH_2 of U or U derivatives was critical to cause the disappearance of the structure that originally formed the N–$(C)_3$ site, destroying its ordered structure. This resulted in the introduction of abundant defects into the skeleton of g-C_3N_4[43]. Ren *et al*. discovered a facile and scalable approach to preparing porous N-deficient g-C_3N_4 via calcination of acetic acid (HAc)-treated melamine as the precursor. The elemental analysis and XPS spectra showed that the N vacancies were introduced and primarily situated at the C-N=C lattice, which was mainly attributed to the imperfect polycondensation of g-C_3N_4 caused by HAc during the pyrolysis process of HAc-treated melamine[44]. To develop an easily con-

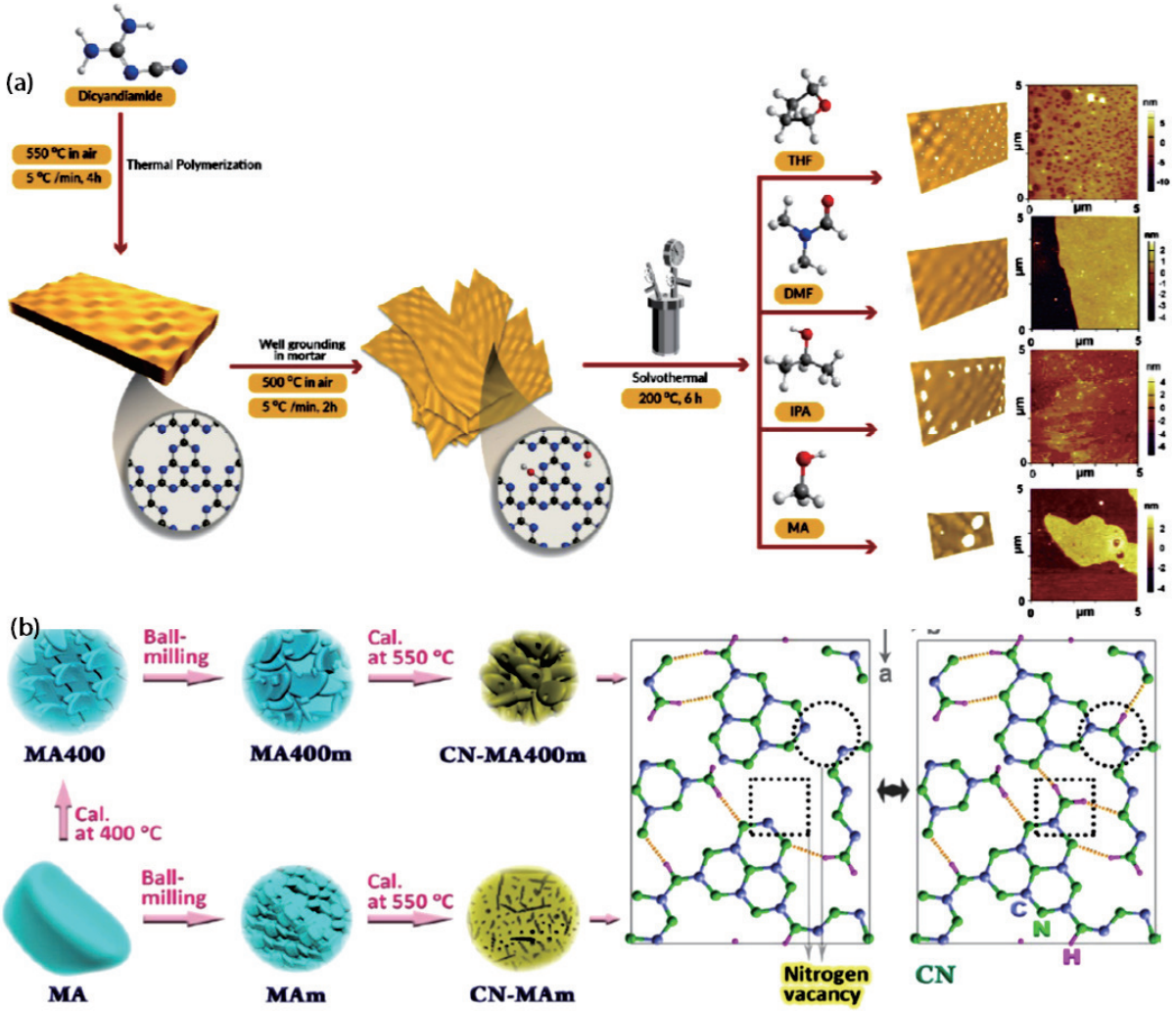

Fig. 6. (Color online) Schematic illustration of the preparation of vacancy-modified g-C_3N_4. The vacancy-modified g-C_3N_4 was prepared via (a) solvothermal treatment of g-C_3N_4-bulk in various organic solvents (Copyright 2022, American Chemical Society)[47], (b) mechanical ball-milling of the intermediate (melem) with succedent calcination (Copyright 2020, American Chemical Society)[52], respectively.

ducted method for preparing nitrogen-deficient g-C_3N_4, Chen *et al*. reported an approach to preparing g-C_3N_4 with N vacancies using acetic acid-treated melamine as a precursor. Their study also found that the –COOH of the acetic acid and the –NH_2 of the melamine could interact at higher temperature, which might weaken and break the chemical bond between the melon unit and NH_2 group, resulting in the release of nitrogen-containing species and forming N vacancies[45].

3.3. Other treatment methods

In addition to these two strategies, many other approaches have been developed for fabricating vacancy-modified g-C_3N_4. In recent years, a solvent-dispersion strategy has been employed to tune the property of g-C_3N_4, wherein organic solvents play an intercalant role in exfoliating the layered precursor of g-C_3N_4 into nanosheets and are employed to generate vacancy defects. This mainly happens because intercalated organic molecules can decompose into gases during the thermal polymerization process, causing some of the atoms on the surface to overflow. As a result, vacancy defects are introduced into the framework of g-C_3N_4[46]. Inspired by this, as shown in Fig. 6(a), Dang *et al*. proposed the *in situ* exfoliation of g-C_3N_4, engineering holey defects on 2D g-C_3N_4 layers via the solvothermal treatment of bulk g-C_3N_4 in various organic solvents (e.g., methyl alcohol, isopropyl alcohol, tetrahydrofuran, and dimethylformamide). It was found that the tetrahydrofuran treatment not only facilitated the formation of a uniform holey structure of g-C_3N_4 but also maintained the lateral size along with N vacancies in the heptazine units[47]. In another study, Huo *et al*. reported a dual strategy that used succinic acid (SA) as the modification agent coupled with a solvent-dispersion strategy to synthesize porous CN nanotubes co-modified with C and defects (N vacancy). During the thermal polymerization process, the addition of succinic acid was helpful to the formation of C modification and the subsequent treatment of solvent (ethanol) dispersion strategy was beneficial to the introduction of N vacancy. This work provided a novel joint strategy for the development of high efficient photocatalyst[48].

The template method is another effective method for preparing vacancy-modified g-C_3N_4. Recently, Liu *et al*. successfully synthesized defects modified mesoporous g-C_3N_4 through a novel thermal polycondensation of the gel from dicyanamide and tetramethoxysilane (TMOS). During the thermal fasculation process, SiO_2 nanoparticles formed from the hydrolysis of TMOS could introduce the formation of mesoporous structure and restrict the thermo-polymerization of dicyandiamine, leading to its incomplete polymerization. As a

result, cyano groups and N vacancy were generated in the skeleton of g-C_3N_4[49]. Recently, a 3D macropore C-vacancy g-C_3N_4 (3DM C/g-C_3N_4) was fabricated via a simple one-step approach, wherein the polymethylmethacrylate spheres were used as a template. Compared to unmodified g-C_3N_4, the photoabsorption region and carrier recombination of the 3DM C/g-C_3N_4 were dramatically optimized due to the introduced C-vacancy[50]. Additionally, mechanochemical methods such as ball-milling mechanochemistry have been widely used to destroy structures and produce defects in materials because they are cleaner, faster, and simpler than traditional strategies[51]. As shown in Fig. 6(b), Ba *et al*. reported a novel mechanochemical method to fabricate mesopore-rich g-C_3N_4 with N vacancies through mechanical ball-milling of the intermediate (melem) with succedent calcination. It was found that the N vacancies and mesopores could be simultaneously introduced into the framework of g-C_3N_4 due to the ball-milling-induced structure distortion and morphological variation of the intermediate[52].

In summary, these works have opened the way for the synthesis of vacancy modified g-C_3N_4 photocatalysts and have provided a new perspective for the synthesis of g-C_3N_4 based photocatalysts with high photocatalytic activity. However, the present methods encounter difficulty in controlling the type, location, and density of vacancy simultaneously. In addition, it is challenging to realize the precise control of vacancy introduction and large-scale preparation. Thus, more accurate and efficient vacancy introduction strategies are desired to fabricate g-C_3N_4 with superior photocatalytic properties.

4. Effect of vacancy defect on photocatalytic water splitting with g-C_3N_4

Vacancy defect engineering has become a widely-adopted strategy to regulate and optimize photocatalytic performance. The missing of N or C atoms reduces the g-C_3N_4 symmetry, while introducing variation in optical, electronic, and surface properties. There has been remarkable progress in g-C_3N_4 defect generation and application in water splitting. Therefore, this section focuses on the effect of vacancy defect in g-C_3N_4 on photocatalytic water splitting and highlights the significance in further utilization.

4.1. Optimizing band structure and enhancing the light absorption

It is commonly known that the excitation from VB to CB is strictly limited by the band gap. Electrons in a semiconductor can only absorb photon energy equal to or greater than bandgap energy, and then participate in migration and reaction. The redox ability of the photocatalyst is dependent on band-edge potential *vs*. NHE. Despite the appropriate potential edges of g-C_3N_4, pristine g-C_3N_4 exhibits poor solar utilization (λ<460 nm) while most solar energy distributes in the visible light and NIR regions[15]. The introduction of vacancy defects is an effective strategy to narrow the bandgap and construct midgap defective states to conquer this shortage. The synergy of the narrowed gap and midgap level can lower excitation requirement and foster the absorption of relatively low-energy photons. The modulated band structure is ascribed to vacancy sites, which can hamper the splitting of bonding and anti-banding orbitals and induce midgap energy states, thus facilitating extended light absorption[14].

Many studies have investigated the effect of vacancy on optimizing band structure and extending light absorption. Huang *et al*. reported nitrogen-vacancies g-C_3N_4 obtained from alkali-supported thermal treatment of melamine (named NVCN)[53]. For insight into the light absorption properties of the samples, UV-vis DRS (Fig. 7(a)) were utilized and the curves indicated the redshift as adding more KOH, which suggested the amelioration in light-harvesting ability. Furthermore, the graphs from $(ahv)^{1/2}$ vs. photon energy showed that there was a steady decrease in band gap at 2.63 eV, leading to enhanced light absorption (Fig. 7(b)). To investigate the effect of vacancy on band structure, Liang *et al*. prepared a series of porous g-C_3N_4 with tunable N-vacancy density by a multi-time heat treatment method[54]. The DRS results showed that the modified g-C_3N_4 sample exhibited extended visible and infrared light absorption as the vacancy density increased (Fig. 7(c)). A new mid conduct band (NMCB) was observed in the Tauc plots and combined with VB XPS, the band structure of samples are depicted in Fig. 7(d). The existence of a midgap state facilitated electron excitation from the VB to easier-reached state and boosted light absorption in visible and infrared region, dramatically elevating the H_2 evolution rate over the pristine sample. In another example, a $N_2H_2{\cdot}H_2O$-assited thermal polymerization was utilized by Wu *et al*. to introduce an N vacancy[55]. Samples named CN-*x* (*x* represented the dose of $N_2H_2{\cdot}H_2O$) displayed enlarged visible-light absorption region and the powder turned to reddish brown as defect density increased (Fig. 8(a)). The band gap energy of CN-500 was decreased to 1.79 eV, which greatly extended the utilization of solar energy. The midgap states originated from vacancy defect showed more negative potential than NHE, which indicated the validity of enriched states for H_2 evolution (Fig. 8(b)). Hence, the photocatalytic activity can be significantly enhanced and the light-harvesting capability is boosted when the band structure is optimized.

To demonstrate the effect of vacancy defect in band structure modulating, Sun *et al*. investigated different vacancies of g-C_3N_4 by the first-principles calculations[56]. Their results revealed that all of the vacancy defects induced a reduction in the band gap, which was consistent with the comprehension of frontier orbital theory. Formation enthalpy analysis suggested the superiority of N2 and C2 vacancy in formation over other vacancies. As shown in Figs. 8(c) and 8(d), the bandgap of the N2 and C2 vacancy defect g-C_3N_4 was obviously narrowed and absorption coefficient curves of defected g-C_3N_4 displayed larger absorption than pristine structure with redshift over the visible wavelength region (380–780 nm). In conclusion, the DFT calculation results showed the effect of vacancy defect on narrowing the bandgap and fostering visible-light absorption, which was consistent with previous reports[19, 54, 55].

4.2. Improving the separation and migration efficiency of photogenerated carriers

Earlier research has shown that the high symmetry of g-C_3N_4 impeded electronic properties and led to a high recombination rate[57]. Similar theoretical results also proved that HOMO and LUMO orbitals were restricted within tri-s-triazine ring structure, so that a small minority of photogenerated carriers reached the surface and took part in goal reactions[58, 59].

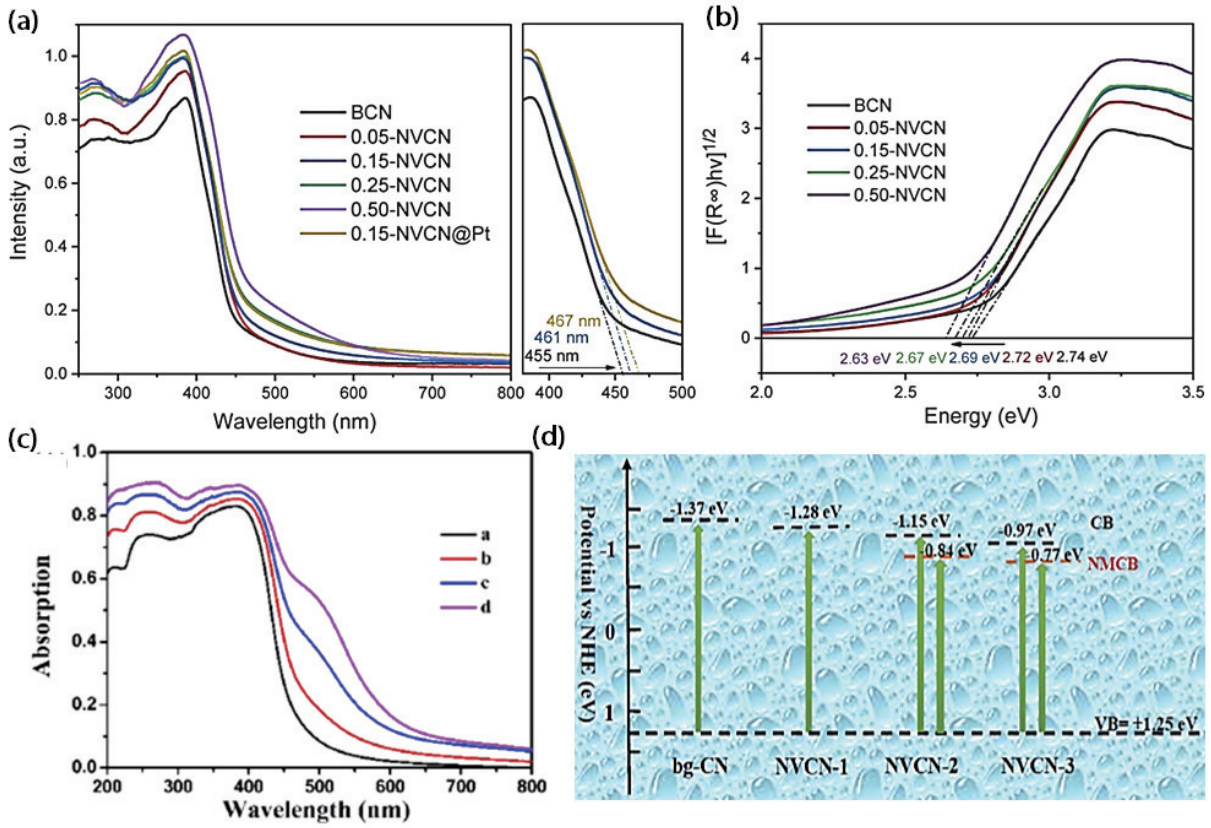

Fig. 7. (Color online) (a) Ultraviolet visible diffuse reflection spectrum(UV-vis DRS) and (b) plots of Kubelka-Munk formula of as-prepared photocatalysts (Copyright 2022, Elsevier)[53]. (c) UV-vis DRS and (d) band structure Illustration of g-C_3N_4 samples with ascending NV concentration (Copyright 2019, Elsevier)[54].

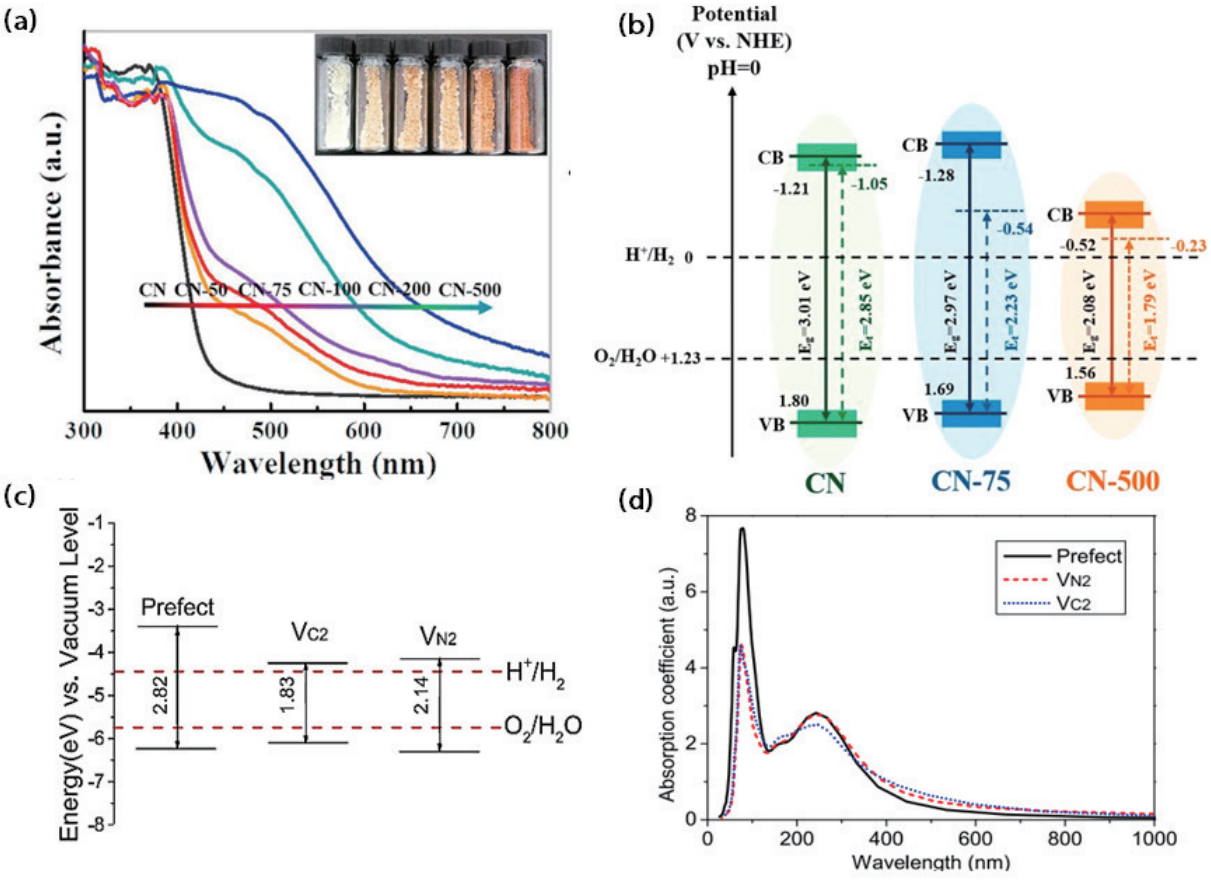

Fig. 8. (Color online) (a) UV-vis DRS of CN-0~500. (b) Illustration of the band structure of three chosen photocatalysts (Copyright 2019, Elsevier)[55]. (c) Diagrams of band structure and (d) absorption coefficient of perfect, C2-defected, N2 defected CN (Copyright 2022, Elsevier)[56].

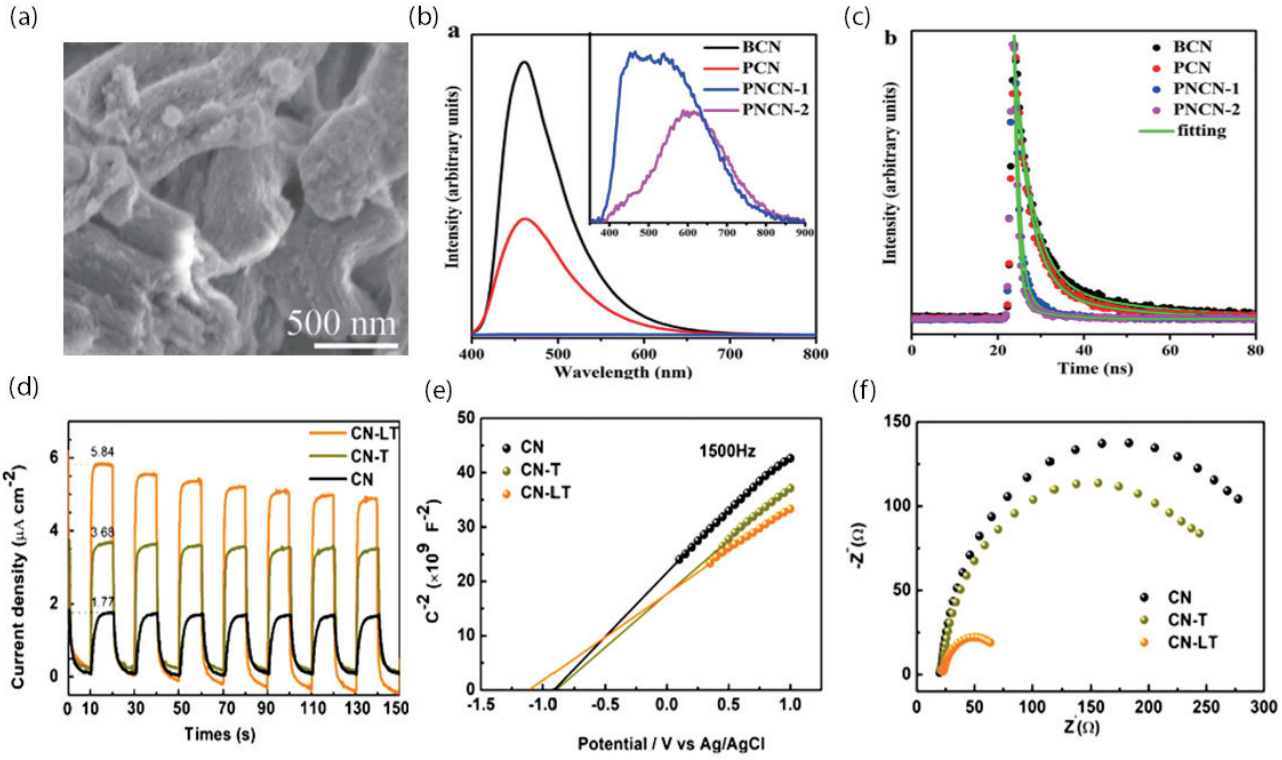

Fig. 9. (Color online) (a) SEM image of PNCN-1. (b) PL spectra and (c) time-resolved PL spectrum of as-developed sample (Copyright 2020, Elsevier)[60]. (d) Photocurrent response diagram, (e) Mott-Schottky plots, (f) EIS Nyquist plots of as-prepared photocatalysts (Copyright 2020, Elsevier)[61].

In this regard, vacancy defects have been considered to be an efficient strategy to reduce symmetry and construct an electron-transfer channel to stimulate the separation and migration of photo-illuminated carriers. In addition, the vacancy may act as electron-trapping center to boost the spatial separation of electron-hole pairs. However, it is also vital to precisely control the distribution and concentration of vacancy because this defect can also act as a recombination center[58]. To investigate the positive role of vacancy on photoexcited carriers separation, Yang *et al*. synthesized N vacancy abundant g-C_3N_4 by hard-template method from dicyandiamide (Fig. 9(a))[60]. The rod-shaped porous g-C_3N_4 was noted as PNCN-x for different processing temperatures. Compared to bulk g-C_3N_4 and the control porous g-C_3N_4 (PCN), the photoluminescence (PL) emission spectra of PNCN displayed a significant decrease in intensity and redshift, which indicated the suppressed recombination of photogenerated carriers and a narrowed bandgap (Fig. 9(b)). For further explanation of the decreased recombination rate, time-resolved photoluminescence (TRPL) spectra were employed to understand the charge-separation kinetics (Fig. 9(c)). PNCN-1, 2 exhibited a much shorter average lifetime of photoexcited carriers than BCN and PCN, which was assigned to the synergy of the shortened interlayer distance and shallow electron-trapping states. The improved separation kinetics and decreased transfer length jointly resulted in the short lifetime of excited electrons, which facilitated the highly efficient separation of photogenerated carriers. Zeng *et al*. modulated g-C_3N_4 by combining LiOH treatment and heat etching, which rendered the vacancy-defected g-C_3N_4 with 19.25 times higher hydrogen evolution reaction (HER) performance than pristine g-C_3N_4[61]. As shown in Fig. 9(d), the modified g-C_3N_4 exhibited the highest transient photocurrent, which was in agreement with its better photocatalytic performance. Moreover, the smaller slope of Mott-Schottky plots and smallest radius of the ESI spectra suggested the modified g-C_3N_4 with higher charge carrier density and the lowest interfacial resistance (Figs. 9(e) and 9(f)). These results revealed that the introduction of N-vacancy defects not only increased the charge carrier density but also reduced the interfacial resistance of the catalyst, thus boosting more electrons to effectively participate in surface reaction.

Considering that vacancy defects can improve the separation and migration efficiency of photogenerated electrons, the construction of heterostructure is also a promising approach to fostering carrier kinetics through interfacial transference[62, 63]. With an appropriate junction structure, vacancy defects can synergistically facilitate the separation and transfer of excited carriers. For instance, Xu *et al*. prepared Co-doped CeO_2 loaded g-C_3N_4 with N vacancies via the self-assembly method[64]. As shown in Fig. 10(a), the excited electrons would be transferred to the Co-CeO_2 with the synergy of the built-in electric field and electron-collecting vacancy defects, while the holes went in the opposite path. The separation efficiency of the prepared heterostructure was dramatically elevated with the joint effect of vacancies and the heterojunction structure. Liao *et al*. reported *in situ* g-C_3N_4 p-n homojunction with plentiful N vacancies via hydrothermal treatment followed by two-step calcinations[65]. The existence of N vacancies resulted in a more positive conduction band and turned the g-C_3N_4 into p-type while the n-type domain was ascribed to ordered g-C_3N_4. As depicted in Fig. 10(b), nitrogen-vacated g-C_3N_4 p-n homojunction structure (NV-g-C_3N_4) exhibited low PL intensity compared to the pristine sample and homojunc-

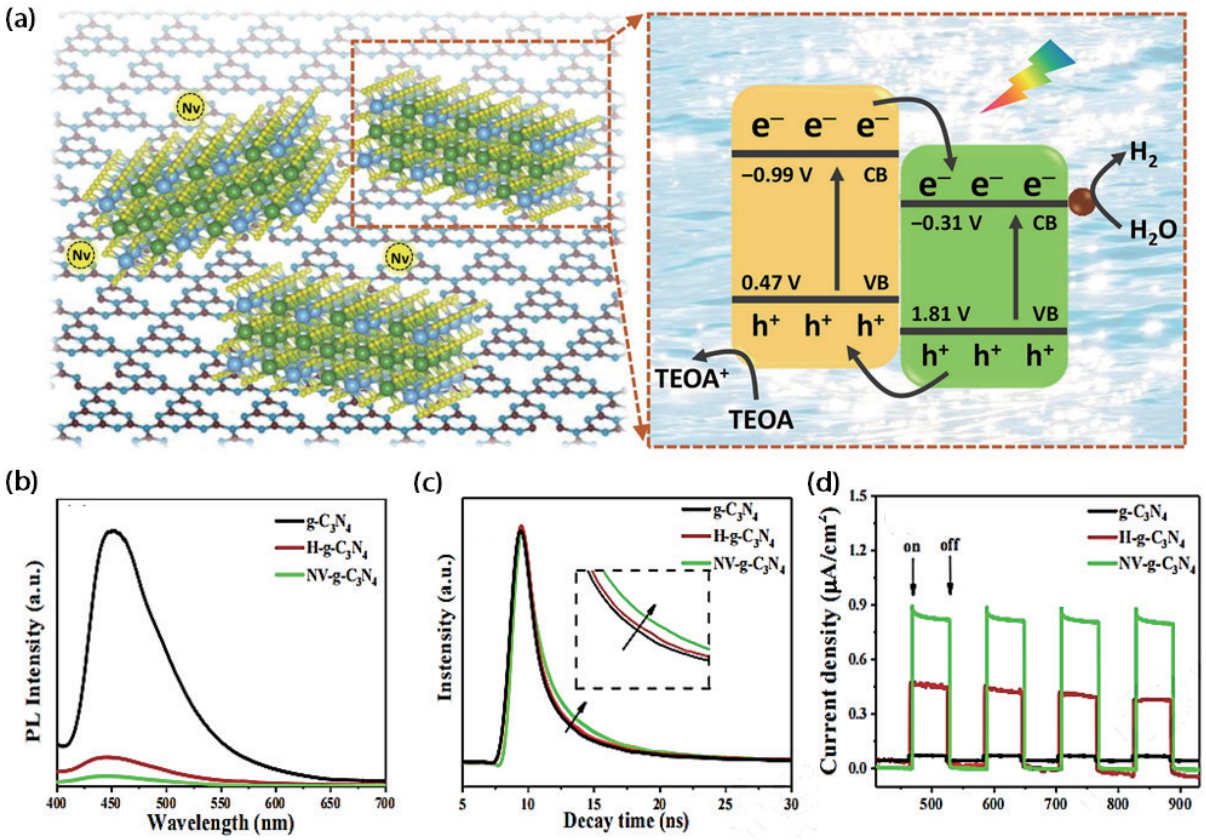

Fig. 10. (Color online) (a) Illustration of the photocatalytic water reduction for as-developed heterojunction (Copyright 2022, Elsevier)[64]. (b) PL spectra, (c) time-resolved PL spectrum, (d) photocurrent response of pristine g-C_3N_4, homojunction and defected homojunction (Copyright 2021, Elsevier)[65].

tion precursor, which suggested that recombination of electron-hole pairs was successfully suppressed. A similar result was found in time-resolved PL spectra that the average lifetime of NV-g-C_3N_4 was 6.78 ns longer than H-g-C_3N_4 (6.52 ns) and pure g-C_3N_4 (5.55 ns) (Fig. 10(c)). Meanwhile, NV-g-C_3N_4 also showed higher photocurrent and lower surface resistance in transient photocurrent response (Fig. 10(d)), which revealed the incremented migration efficiency of photo-induced carriers. Consequently, the recombination of photo-generated carriers was efficiently hindered, and more electrons and holes became available in the surface reaction.

4.3. Enhancing the surface water splitting reaction kinetics

Surface reaction kinetics are another restraining factor for rapid photocatalytic reaction and efficient solar utilization, and vacancy defects also have effects on enhancing the surface reaction kinetics. It has been found that vacancy defects can increase the surface area. When combined with porous structure, g-C_3N_4 could obtain a significantly enlarged surface area[66]. As a result of the expanded surface area, more active sites are exposed for incremented water splitting. Moreover, the appropriate design of surface defects can enhance the absorption of molecules to accelerate the reaction process with better mass transfer. The deformation charge density (DCD) calculations of C_{V2} vacancy showed that the electron density appeared to be higher at vacancy sites (Fig. 11(a))[67]. Thus, surface C vacancy is in favor of H^+ chemisorption and has the potential to act as active sites for water splitting. In another example, Yao *et al*. reported that the vacancy defect generation not only endowed g-C_3N_4 with more surface-active sites but also remarkably ameliorates surface kinetics. As a result, the photocatalytic H_2 evolution rate of the N vacancy-defected g-C_3N_4 was improved from none to 10.12 μmol/(g·h) without any cocatalyst modification[68].

A large-surface structure would take full advantage of the vacancy defect for a further increase of the special surface area. Liang *et al*. adopted thermal post-treatment to obtain g-C_3N_4 nano-fragments with N vacancies[69]. The ultrathin and porous structure reduced carrier recombination and induced an enlarged surface area with more active sites exposed. As a result, Nano-CN5 was obtained with 10 h heat etching, which had a thickness of 2.7 nm under AFM investigation, a Brunauer-Emmette-Teller (BET) surface area of 57.65 m^2/g, and 11 folds as a pristine sample. In another example, Zhang *et al*. synthesized ultrathin g-C_3N_4 nanosheets with N vacancies (CN-UNS) using a well-designed thermal exfoliation method (Fig. 11(b)). The nanosheets exhibited dramatically enhanced HER performance[70]. The synergy of thermal exfoliation and defect engineering constructed nanosheets that were stacked in three layers (Fig. 11(c)), which largely reduced the transport distance of excited electrons for surface reaction. The N_2 adsorption-desorption test of CN-UNS illustrated type IV with a hysteresis loop, which indicated its mesoporous structure. The BET surface area of CN-UNS was about 35.3 folds that of CN and the pore radius distribution suggested a well-designed porous structure (Fig. 11(d)). With much more active sites exposed, a strengthened ability of light absorption, and charge carrier separation, CN-UNS exhibited high photocatalytic activity when compared to pristine

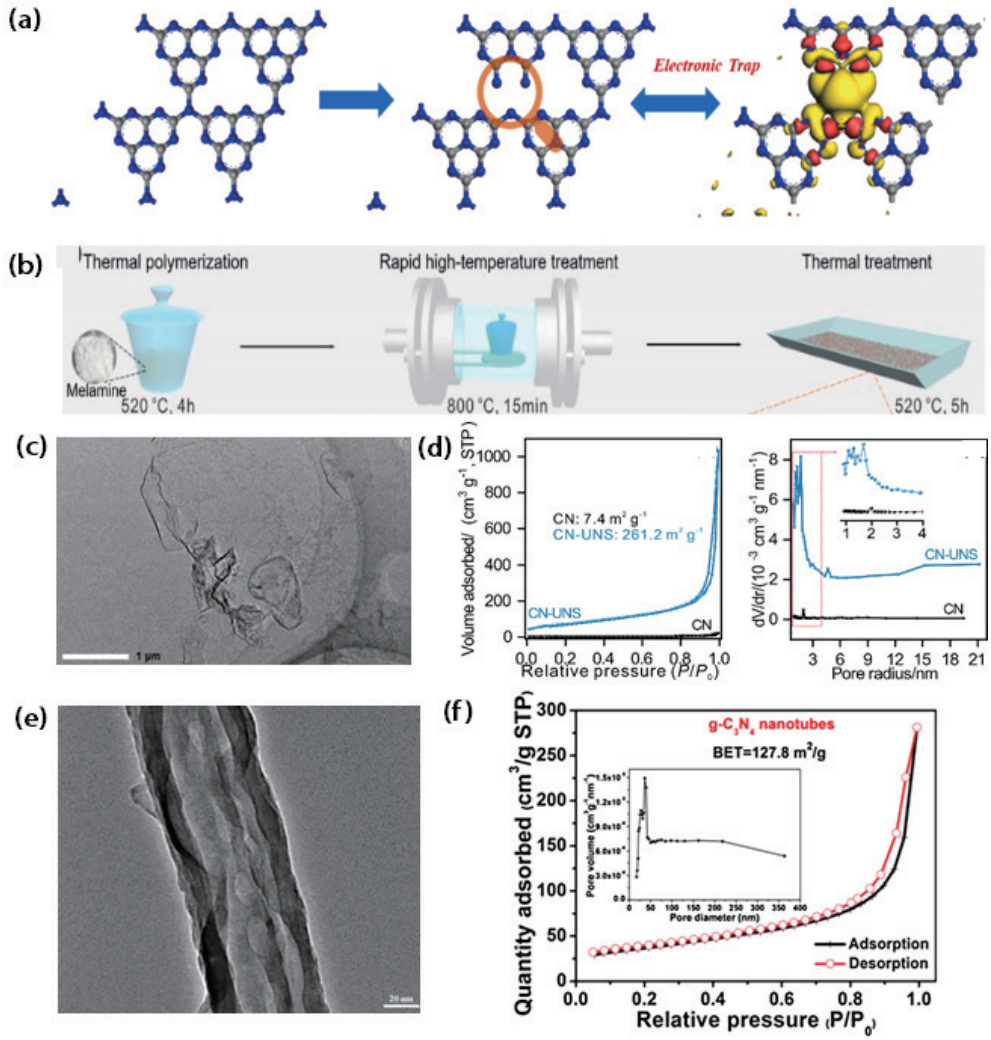

Fig. 11. (Color online) (a) A schematic of perfect (i), C_{V2}-defected g-C_3N_4 (ii) structure and the electron trap (iii) in defected structure (Copyright 2021, Elsevier)[67]. (b) A schematic of heat-exfoliation synthetic route of the N-defected photocatalyst. (c) A TEM image of the CN-UNS. (d) A nitrogen absorption-desorption isotherm and the pore distribution diagram of the CN-UNS (Copyright 2022, Elsevier)[70]. (e) A SEM image and (f) nitrogen absorption-desorption isotherm of the as-prepared g-C_3N_4 nanotubes (Copyright 2018, Elsevier)[71].

g-C_3N_4. Additionally, Mo *et al*. reported an acid-alkali-free method for synthesizing g-C_3N_4 nanotubes with abundant N vacancies[71]. With a wall thickness of 15 nm (Fig. 11(e)), the tubular structure could not only access extended light absorption with extra reflection or scattering but also realize a fine control of stacking, which was beneficial for a large surface area. As shown in Fig. 11(f), the BET surface of the nanotubes was significantly enlarged, which demonstrates an efficient strategy to extend surface area with the synergy of vacancy defects. As a whole, vacancy defect engineering is an effective and inclusive strategy to activate surface reaction kinetics with ameliorated reaction sites and increased surface area.

5. Vacancy-modified g-C_3N_4 for solar water splitting

Band structure is not only the significant factor for light-harvesting ability but also dominates the redox capability of the catalyst over multifarious reactions. Considering the suitable band-edge position of g-C_3N_4 for overall water splitting reaction, global researchers have made a lot of progress in optimizing the photocatalytic activity of g-C_3N_4 by vacancy defect modification in overall water splitting, for purely hydrogen or oxygen evolution. By using vacancy defect engineering, ameliorated optical, electrical, and reaction kinetic properties could be expected.

5.1. Overall water splitting

Photocatalytic overall water splitting (OWS) involves four electrons in an uphill process in demand of a Gibbs free energy of 237 kJ/mol, which is equal to 1.23 eV[22]. In detail, the band-edge potentials of the target photocatalyst are expected to straddle the potential of H_2 evolution and O_2 evolution to meet the redox capability requirements. Moreover, in consideration of the molecular kinetic viewpoint, the reaction barrier in the two half reactions means that a larger bandgap is in favor of OWS. However, the fact that over 94% of the total solar radiation energy is distributed in the visible-light and infrared region favors a narrower bandgap for a better light-harvesting ability[14]. Nonetheless, it is a great challenge to achieve efficient OWS without any sacrificial reagent, which is known as the “holy grail” of solar energy utilization[72, 73]. Therefore, an efficient OWS system with fine stability is still an urgent desire for researchers.

To ameliorate the band structure of g-C_3N_4 and construct an efficient OWS system, Shao *et al*. developed an

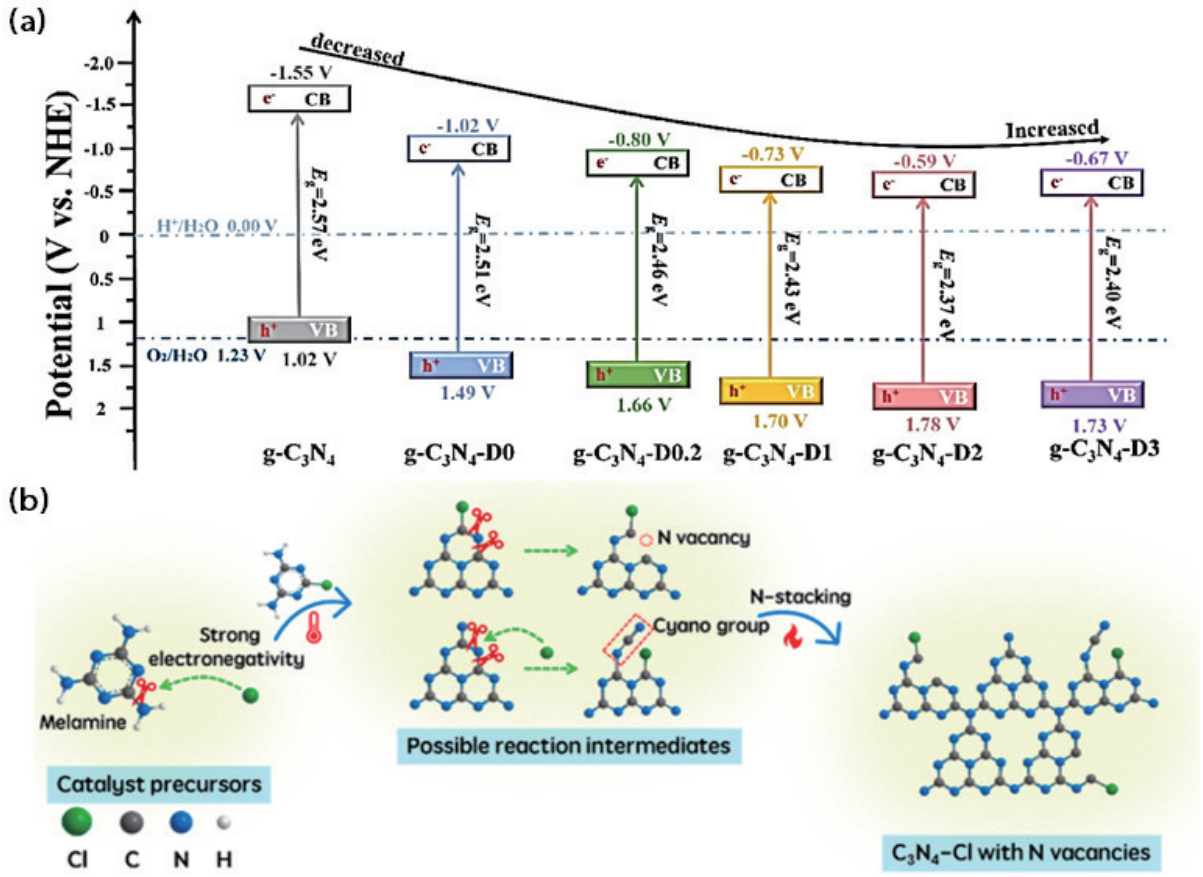

Fig. 12. (Color online) (a) Band structures of the defected photocatalyst series (Copyright 2023, Elsevier)[37]. (b) The illustration of the defect introduction process with Cl^- (Copyright 2022, ACS Publications)[74].

alkali-assisted molten salt method[37]. As shown in Fig. 12(a), the band structure of g-C_3N_4 could be tuned by altering the N-vacancy concentration with KOH, and g-C_3N_4-D2 showed the lowest charge transfer resistance and the highest photocatalytic activity. As a result, after dual cocatalyst loading, the vacancy-modified compound system showed efficient OWS performance with H_2 evolution rate, 49.60 μmol/(g·h), and O_2 evolution rate, 24.71 μmol/(g·h). In another work, Zhang *et al*. adopted a tunable and facile vacancy generation method and achieved an apparent quantum yield of 6.9% at 420 nm, which was the highest for g-C_3N_4 OWS performance[74]. For insight into the vacancy formation process, the DFT calculation was adopted and the results revealed that the formation energy of N_{2C} vacancy was reduced by 21% with Cl^- regulation, while that of N_{3C} vacancy was 5% lower, which caused the superiority of N_{2C} vacancy formation (Fig. 12(d)). The g-C_3N_4-Cl_x sample exhibited thinner stacking and larger BET special surface area than pristine g-C_3N_4. As a result, g-C_3N_4-Cl_4 showed a rate of 48.2 μmol/h for hydrogen production and 21.8 μmol/h for oxygen production. The incremented OWS rate was attributed to the selectively constructed vacancy defects and the significantly enhanced carrier separation efficiency.

5.2. Hydrogen evolution

Considering the easily-realized higher hydrogen evolution rate compared to that of OWS, photocatalytic partial water splitting (PPWS) has been the most widely researched approach for solar hydrogen production, despite the cost of the sacrificial agent[75]. A sacrificial reagent captures the photogenerated holes, fostering the evolution rate of hydrogen. Triethanolamine (TEOA) has been widely chosen for this role. Vacancy defect construction in g-C_3N_4 is able to boost the light absorption capability and facilitate the separation of the photogenerated carriers[58]. In addition, vacancy engineering can be jointly combined with morphology control, element doping, and heterojunction construction for an elevated hydrogen evolution rate. The vacancy defect g-C_3N_4 performance of recent studies is summarized in Table 1.

To make full use of the advantage of synergic modification, Huo *et al*. employed C insertion and N-vacancy defects by means of succinic acid and solvent-dispersion process, respectively[48]. The redshift effect of introduced C and the midgap defect state synergistically enlarged the light absorption range of g-C_3N_4 (Fig. 13(a)), which enhanced the n-π^* transition with a decreased crystallinity and higher delocalized electron density. DFT calculations on the double-modified sample indicated that both of the modifications caused an increase in charge density around adjacent N atoms, which was beneficial to the separation of electron-hole pairs. Coupled with the increased surface area, the nanotubes exhibited a high stability and outstanding HER performance (Fig. 13(b)). Moreover, as illustrated in Fig. 13(c), Zhang *et al*. adopted a facile thermal reduction treatment to form porous g-C_3N_4 granule with rich C vacancies[76]. They revealed that the C defects constructed adjacent to the bridge N atoms reduced the bandgap by 0.41 eV, which synergistically added to the light absorption with the interior scattering of the porous structure. Moreover, the more negative conduction band minimum (CBM) added to the advantage of C-vacancy

Table 1. Representative summary of vacancy-defected g-C_3N_4 photocatalyst for H_2 production.

Year	Photocatalyst	Cocatalyst (%)	Illumination condition	Reaction solution (vol%)	HER (μmol/(g·h))	AQY (%) (wavelength)	Stability (h)	Ref.
2021	N-deficient g-C_3N_4	Pt wt	300 W Xe lamp	Methanol 20 vol	287.94	3.06 (420 nm)	12	[68]
2021	Porous N-deficient g-C_3N_{4v} nanotubes	Pt wt 3	425 mW/cm^2 $\lambda \geqslant 420$ nm	TEOA 10	8.52×10^3	5.6 (420 nm)	64	[48]
2021	Granular C-deficient g-C_3N_4 nanotubes	Pt wt 1	300 W Xe lamp	Methanol 20	3281.2	_	18	[76]
2021	C-deficient g-C_3N_4 nanosheets	Pt wt 3	300 W $\lambda \geqslant 420$ nm	TEOA 10	1.86×10^3	_	16	[80]
2022	Ultrathin porous g-C_3N_4 nanosheets with N vacancy	Pt wt 3	300 W $\lambda \geqslant 420$ nm	TEOA 10	5.74×10^3	14.9 (420 nm)	18	[70]
2020	Porous and thin-layered g-C_3N_4 with N vacancy	Pt wt 3	300 W $\lambda \geqslant 420$ nm	TEOA 20	1.557×10^3	11.2 (420 nm)	20	[18]
2021	Porous g-C_3N_4 nanosheets with C and N vacancies	Pt wt 1	100 mW/cm^2 365~940 nm	TEOA 10	297.6	12.7 (420 nm)	20	[81]
2021	N-O double vacancy defected g-C_3N_4	Pt wt 3	300 W $\lambda \geqslant 420$ nm	TEOA 10	595	_	20	[79]
2020	O-doped and N-defected g-C_3N_4	Pt wt 3	300 W $\lambda \geqslant 420$ nm	TEOA 10	2.20×10^3	9.19 (420 nm)	20	[77]
2022	S-doped and N-defected mesoporous g-C_3N_4	Pt wt 1.5	300 W $\lambda \geqslant 400$ nm	TEOA 5	4.441×10^3	6.8 (420 nm)	12	[78]
2022	Carbon species inserted g-C_3N_4 with N vacancy	Pt wt 2	300 W AM 1.5 G	TEOA 10	1.4582×10^4	6.98 (420 nm)	15	[82]
2023	Crystalline g-C_3N_4 with N vacancy	Co_3O_4 wt 3 Pt wt 1	300 W $\lambda \geqslant 420$ nm	Lactic acid 10	3.78×10^3	11.94 (400 nm)	15	[37]
2022	N-deficient g-C_3N_4 hybridized with Cu_2O	Pt wt 3	350 W $\lambda \geqslant 400$ nm	TEOA 30	420.3	0.87 (420 nm)	12	[83]
2022	Ni-Co NP modified N-deficient g-C_3N_4 nanotubes	_	300 W $\lambda \geqslant 420$ nm	TEA 30	205.5	_	16	[84]
2023	N-deficient g-C_3N_4/NiO heterojunction	_	300 W Xe lamp	TEOA 15	169.5	_	16	[85]
2023	N-deficient g-C_3N_4/CdS heterojunction	Ag wt 0.4	300 W $\lambda \geqslant 420$ nm	TEOA 10	204.19	3.94 (450 nm)	16	[86]

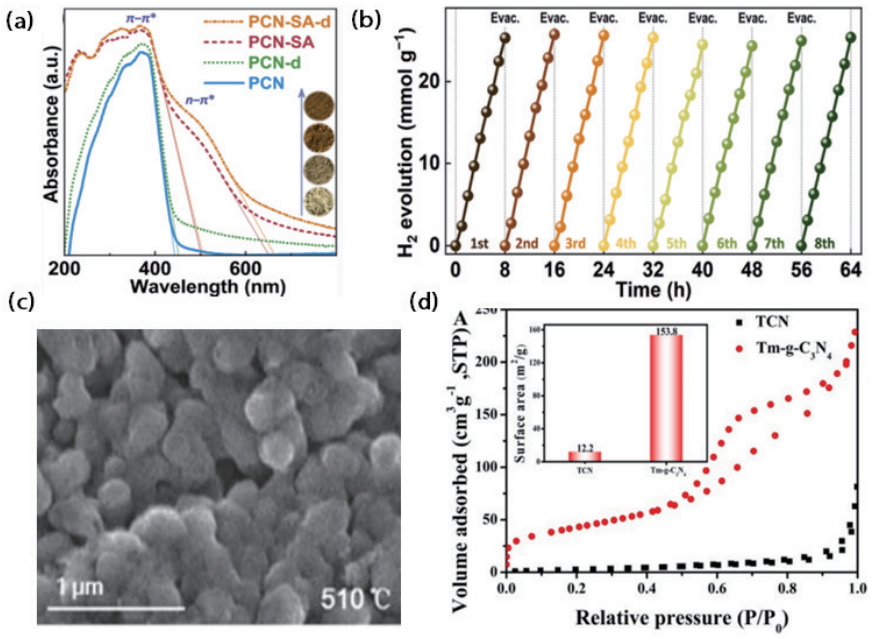

Fig. 13. (Color online) (a) UV-vis DRS of as-prepared photocatalysts. (b) The stability test of the g-C_3N_4 nanotube photocatalyst (Copyright 2021, Elsevier)[48]. (c) The nitrogen absorption-desorption isotherm of the S-doped and N-deficient g-C_3N_4 (Copyright 2022, Elsevier)[78]. (d) SEM image of granular g-C_3N_4 obtained at 510 °C (Copyright 2021, Wiley Online Library)[76].

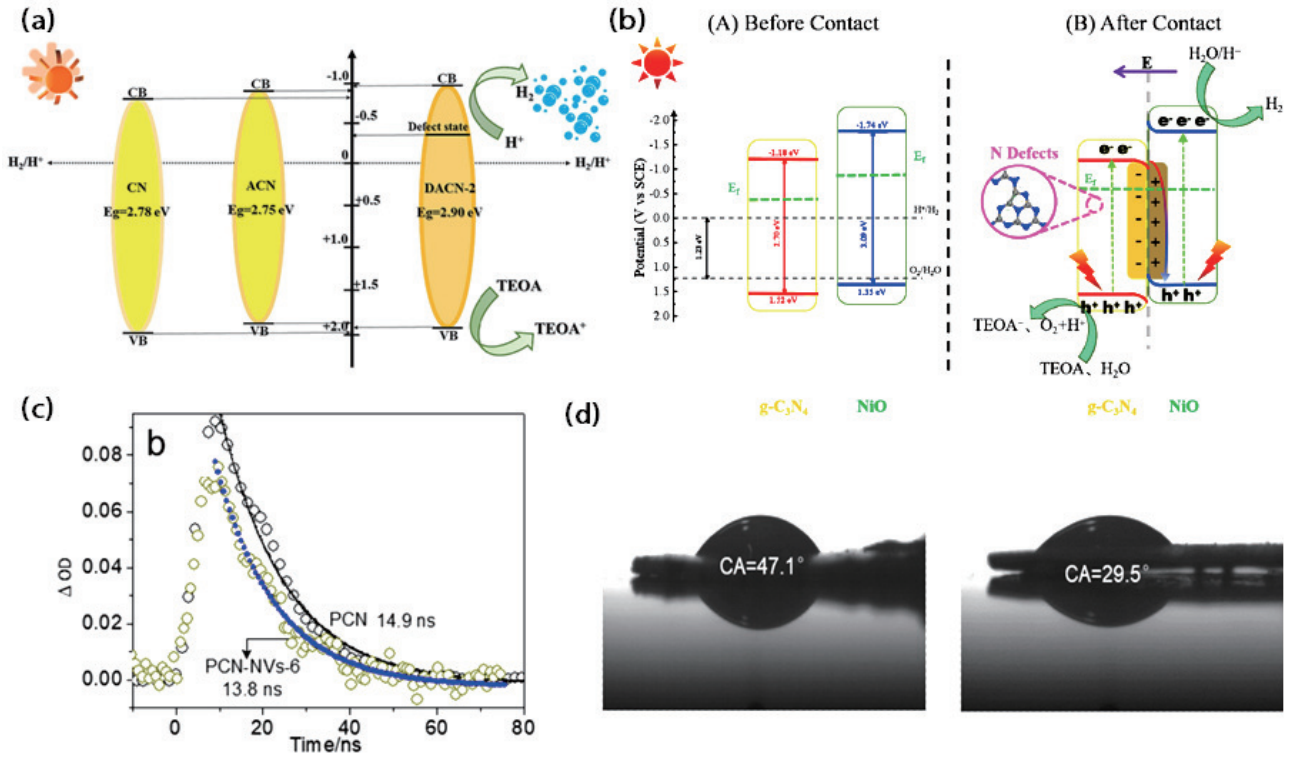

Fig. 14. (Color online) (a) The band structure and hydrogen evolution mechanism of the as-developed photocatalysts (Copyright 2021, Elsevier)[79]. (b) The band structure and S-scheme photocatalytic mechanism of the hybridization (Copyright 2023 Elsevier)[85]. The TAS plots (c) and contact angle measurements (d) of PCN and N-defected PCN (Copyright 2019, Elsevier)[39].

defects with enhanced reducing capacity. In another example, urea-controlled thin-layer stacking with N defects was constructed with an alkali-assisted method by our group[18]. Besides N defects, the synergy of urea and KOH introduced affluent cyano groups, which jointly reduced the bandgap to 1.81 eV. The thickness of the stack was remarkably reduced to around 10 nm, while the mesopore structure was endowed after alkali etching. The rational modification of morphology created sufficient exposure for abundant active sites enriched by N vacancies. Generally, a thinner layer and more pores would lead to quicker separation of photogenerated electrons and holes. Thus, the obtained sample displayed remarkably enhanced photocatalytic HER performance.

The combination of element doping and vacancy generation is also regarded as an auspicious strategy to enhance photocatalytic HER performance[77]. For instance, Liu *et al*. synthesized S-doped and N-defected g-C_3N_4 through a hard-template method[78]. The as-prepared sample displayed a reduced bandgap and a more negative CBM level compared to single S-doped g-C_3N_4, which was beneficial for photo absorption and proton reduction half reaction. In particular, the layered structure possessed a high BET surface area of 153.8 m^2/g (Fig. 13(d)) and 12.6 folds as the directly calcined sample. As a result, Tm-g-C_3N_4 exhibited high photocatalytic activity, which was 48.8 times more than the HER performance of the previous sample. In a recent report, Lin *et al*. developed an enhanced N defect engineering strategy by oxygen doping[79]. The bandgap of the obtained sample (DACN) was extended and a defect state was observed near CB (Fig. 14(a)), which facilitated the light-harvesting capacity. The rich N defects and residual O atoms jointly contributed to the π-delocalized electron density, fostering the carrier transfer and separation efficiency. As a result, a 11.7 times incremented HER performance was achieved. The dual modification strategy provided a flexible vacancy engineering case for future research.

The heterojunction structure is profiled to be an effective supplement to vacancy defect generation[16]. In an article by Zhu *et al*., bimetallic Ni-Co nanoparticles were loaded to N-deficient g-C_3N_4 nanotubes with a fine Schottky contact[84]. The combination of the two transition metals improved mutual stability and acted as an electron collector, facilitating charge separation. The N vacancy synergistically enhanced the electron transformation from g-C_3N_4 to Ni-Co nanoparticles, where water reduction took place. Therefore, an efficient hydrogen evolution system without a Pt cocatalyst was constructed. In a very recent article, Li *et al*. developed a NiO/g-C_3N_4 S-scheme system with N-vacancy generation[85]. The NiO segment was an oxidative photocatalyst (OP), while g-C_3N_4 was a reductive photocatalyst (RP). The discrepancy between Fermi levels induced band bending (Fig. 14(b)), which drove relatively low-energy electrons and holes to recombine. Hence, spatial-separated electrons and holes with stronger redox capability were available for target reactions. The synergy of the defective electron-trapping center and the interior electric field endowed the system with ameliorated charge-separation efficiency. As a whole, a high-efficiency H_2 production S-scheme system assisted by transition metal oxide was built.

5.3. Oxygen evolution

The effective photocatalytic system for oxygen evolution reaction (OER) has been the common pursuit among solar utilization researchers because the sluggish OER kinetics affects the efficient overall water splitting reaction[87]. To investigate the role of N vacancy on OER, Yang *et al*. reported surface N-

vacancy modification on PCN by a photocarving method[88]. The introduced surface vacancy contributed to visible-light absorption and redistributed the π-conjugated electrons around the defect sites. Moreover, the transient absorption spectroscopy (TAS) results indicated the hole trapper effect of N vacancies (Fig. 14(c)) and the contact angle tests revealed enhanced water absorption after modification (Fig. 14(d)), which improved the electron-hole separation efficiency and mass diffusion. As a whole, the N vacancy has a positive effect on the water oxidation process.

The hybridization strategy between defected g-C_3N_4 and other OER photocatalysts is also valued for synergistically fostered oxygen evolution[16]. Yang *et al*. fabricated a Z-scheme photocatalytic system of Ag_3PO_4/g-C_3N_4 modified with N-vacancy defects, obtaining an optimized OER of 228.8 μmol/(g·h) without cocatalyst[89]. The alkali-assisted introduction of N defects led to a porous interconnected morphology. The Ag_3PO_4 nanoparticles were loaded after *in situ* chemical deposition with new bonds such as C–O, C–OH formed, indicating the tight interfacial contact between Ag_3PO_4 and g-C_3N_4, and the ameliorated interfacial electron transfer. The hybridization constructed a Z-scheme carrier transformation in which the hot holes in the VB of Ag_3PO_4 and the excited electrons in the CB of g-C_3N_4 participated in water splitting. The composite photocatalytic heterojunction took advantage of the single components with synergetic effect of significantly facilitated charge separation.

The absence of relatively high-efficiency OER photocatalyst compared to progress in HER has, however, blocked the development of overall water splitting[90], which may be intuitively disclosed by the number of recent articles. Moreover, the costly sacrificial agents and related poor stability are also dilemmas faced by OER photocatalyst development[88]. An efficient, stable, and inexpensive photocatalytic oxygen evolution system is urgently required for a breakthrough in this field.

6. Conclusion and future perspectives

In this review, we have summarized the fabrication strategies, effect of vacancy generation in g-C_3N_4 on its photocatalytic performance, and the recent developments of vacancy-modified g-C_3N_4 for solar water splitting. Specifically, thermal treatment and chemical treatment are two main strategies to fabricate vacancy-modified g-C_3N_4. Vacancy defects in g-C_3N_4 have an obvious influence on its photocatalytic performance by generating midcap states and regulating its band structure to improve light harvesting. Moreover, vacancy defects serve as effectual shallow capturing sites for charge carriers and photocatalytic reagents during solar water splitting reactions, which can remarkably improve the separation and migration efficiency of photogenerated carriers, and can enhance the surface water splitting reaction kinetics. As a result, numerous vacancy-modified g-C_3N_4 based photocatalysts have been developed for solar water splitting.

Although considerable progress of vacancy-modified g-C_3N_4 has been achieved, there are some trends and challenges remaining under fabrication, characterization, and application of vacancy-modified g-C_3N_4, which are discussed in the following:

(1) As summarized earlier, many strategies have been developed to prepare vacancy-modified g-C_3N_4. However, it is still difficult to simultaneously control the type, quantity, and exact location of the vacancy defect through the existing synthetic routes. Moreover, the present approaches make it difficult to achieve large-scale production of defective g-C_3N_4. Therefore, approaches that can synergistically control different properties of vacancy defects and successfully achieve mass production need to be developed further.

(2) Despite the development of vacancy defect engineering, the relationship and interaction mechanism between the vacancy defects and activity of modified g-C_3N_4 are still huge challenges. More powerful characterization techniques and advanced calculation theories are imperative for detecting the association between vacancies and photocatalytic performance, simulating, and guiding the experimental work, investigating the intrinsic interaction mechanism, and for our in-depth understanding of defects.

(3) Although g-C_3N_4 has strong physicochemical stability, the reproducibility and stability of vacancy-modified g-C_3N_4 are often ignored, and the key factors that control stability have not been thoroughly studied. However, the reproducibility and stability of photocatalysts are crucial for practical photocatalytic reactions. Therefore, more and deeper experimental and theoretical investigations of the stability of vacancy defects modified g-C_3N_4 should be of concern for future research.

(4) Various strategies have been employed to optimize the property of g-C_3N_4, such as morphology engineering, construction of heterojunction structure, heteroatom doping, crystallinity modulation and synthesis of a new molecular structure. Nevertheless, the approaches that combine vacancy defect engineering with other regulatory strategies to precisely tune the different features of g-C_3N_4 need to be researched further, which would be a promising direction for preparing efficient and versatile g-C_3N_4-based photocatalysts.

It is certain that the synergic development of defect design, synthesis, and characterization will further promote the application of vacancy-modified g-C_3N_4 in the field of photocatalysis, such as solar water splitting, photocatalytic CO_2 reduction, bacterial disinfection, and degradation of organic pollutants. It can also facilitate the development of a new generation of g-C_3N_4 based photocatalysts for environment and energy-related applications. Overall, thanks to the continuous efforts of scientists all over the world, there is an exciting and brightening future for g-C_3N_4-based nanomaterials.

Acknowledgements

This work is supported mainly by the National Key Research and Development Program of China (Grant No. 2018YFE0204000), the National Natural Science Foundation of China (Grant Nos. 21975245, U20A20206, 51972300, 12004094, and 32101004), the Strategic Priority Research Program of the Chinese Academy of Sciences (Grant No. XDB43000000), the Science and Technology Research and Development Program of Handan (Grant No. 21422111246). Prof. Y. Huang. also acknowledges the support from the Doctoral Special Fund Project of Hebei University of Engineering. Prof. K. Liu. appreciates the support from Youth Innovation Promotion Association, the Chinese Academy of Sciences (Grant No. 2020114), and the Beijing Nova Program (Grant No.

2020117), Guangdong Basic and Applied Basic Research Foundation (Grant No. 2022A1515110578).

References

[1] Tao X, Zhao Y, Wang S, et al. Recent advances and perspectives for solar-driven water splitting using particulate photocatalysts. Chem Soc Rev, 2022, 51(9), 3561

[2] Staffell I, Scamman D, Velazquez Abad A, et al. The role of hydrogen and fuel cells in the global energy system. Energy Environ Sci, 2019, 12(2), 463

[3] Fujishima A, Honda K. Electrochemical photolysis of water at a semiconductor electrode. Nature, 1972, 238(5358), 37

[4] Li C, Li J, Huang Y, et al. Recent development in electronic structure tuning of graphitic carbon nitride for highly efficient photocatalysis. J Semicond, 2022, 43(2), 021701

[5] Navalón S, Dhakshinamoorthy A, Álvaro M, et al. Metal–organic frameworks as photocatalysts for solar-driven overall water splitting. Chem Rev, 2023, 123(1), 445

[6] Wang Z, Li C, Domen K. Recent developments in heterogeneous photocatalysts for solar-driven overall water splitting. Chem Soc Rev, 2019, 48(7), 2109

[7] Ganguly P, Harb M, Cao Z, et al. 2D nanomaterials for photocatalytic hydrogen production. ACS Energy Lett, 2019, 4(7), 1687

[8] Faraji M, Yousefi M, Yousefzadeh S, et al. Two-dimensional materials in semiconductor photoelectrocatalytic systems for water splitting. Energy Environ Sci, 2019, 12(1), 59

[9] Ong W J, Tan L L, Ng Y H, et al. Graphitic carbon nitride ($g\text{-}C_3N_4$)-based photocatalysts for artificial photosynthesis and environmental remediation: are we a step closer to achieving sustainability. Chem Rev, 2016, 116(12), 7159

[10] Liao G, Gong Y, Zhang L, et al. Semiconductor polymeric graphitic carbon nitride photocatalysts: the "holy grail" for the photocatalytic hydrogen evolution reaction under visible light. Energy Environ Sci, 2019, 12(7), 2080

[11] Lin L, Yu Z, Wang X. Crystalline carbon nitride semiconductors for photocatalytic water splitting. Angew Chem Int Ed, 2019, 58(19), 6164

[12] Lau V W, Lotsch B V. A tour-guide through carbon nitride-land: structure- and dimensionality-dependent properties for photo(electro)chemical energy conversion and storage. Adv Energy Mater, 2022, 12(4), 2101078

[13] Fu J, Zhu B, Jiang C, et al. Hierarchical porous O-doped $g\text{-}C_3N_4$ with enhanced photocatalytic CO_2 reduction activity. Small, 2017, 13(15), 1603938

[14] Kumar A, Raizada P, Hosseini-Bandegharaei A, et al. C-, N-Vacancy defect engineered polymeric carbon nitride towards photocatalysis: viewpoints and challenges. J Mater Chem A, 2021, 9(1), 111

[15] Yang J, Wang H, Jiang L, et al. Defective polymeric carbon nitride: Fabrications, photocatalytic applications and perspectives. Chem Eng J, 2022, 427, 130991

[16] Yu X, Ng S F, Putri L K, et al. Point-defect engineering: leveraging imperfections in graphitic carbon nitride ($g\text{-}C_3N_4$) photocatalysts toward artificial photosynthesis. Small, 2021, 17(48), 2006851

[17] Ruan D, Kim S, Fujitsuka M, et al. Defects rich $g\text{-}C_3N_4$ with mesoporous structure for efficient photocatalytic H_2 production under visible light irradiation. Appl Catal, B, 2018, 238, 638

[18] Huang Y, Liu J, Zhao C, et al. Facile synthesis of defect-modified thin-layered and porous $g\text{-}C_3N_4$ with synergetic improvement for photocatalytic H_2 production. ACS Appl Mater Interfaces, 2020, 12(47), 52603

[19] Li S, Dong G, Hailili R, et al. Effective photocatalytic H_2O_2 production under visible light irradiation at $g\text{-}C_3N_4$ modulated by carbon vacancies. Appl Catal B, 2016, 190, 26

[20] Xu X, Xu Y, Liang Y, et al. Vacancy-modified $g\text{-}C_3N_4$ and its photocatalytic applications. Mater Chem Front, 2022, 6(21), 3143

[21] Takata T, Domen K. Particulate photocatalysts for water splitting: Recent advances and future prospect. ACS Energy Lett, 2019, 4(2), 542

[22] Wang Q, Domen K. Particulate photocatalysts for light-driven water splitting: mechanisms, challenges, and design strategies. Chem Rev, 2020, 120(2), 919

[23] Kim J H, Hansora D, Sharma P, et al. Toward practical solar hydrogen production–an artificial photosynthetic leaf-to-farm challenge. Chem Soc Rev, 2019, 48(7), 1908

[24] Huang Y, Liu J, Deng Y, et al. The application of perovskite materials in solar water splitting. J Semicond, 2020, 41(1), 011701

[25] Kumar S, Karthikeyan S, Lee A F. $g\text{-}C_3N_4$-based nanomaterials for visible light-driven photocatalysis. catalysts, 2018, 8(2), 74

[26] Bai S, Zhang N, Gao C, et al. Defect engineering in photocatalytic materials. Nano Energy, 2018, 53, 296

[27] Niu P, Qiao M, Li Y, et al. Distinctive defects engineering in graphitic carbon nitride for greatly extended visible light photocatalytic hydrogen evolution. Nano Energy, 2018, 44, 73

[28] Niu P, Liu G, Cheng H M. Nitrogen vacancy-promoted photocatalytic activity of graphitic carbon nitride. J Phys Chem C, 2012, 116, 11013

[29] Han Q, Cheng Z, Wang B, et al. Significant enhancement of visible-light-driven hydrogen evolution by structure regulation of carbon nitrides. ACS Nano, 2018, 12(6), 5221

[30] Niu P, Yin L C, Yang Y Q, et al. Increasing the visible light absorption of graphitic carbon nitride (Melon) photocatalysts by homogeneous self-modification with nitrogen vacancies. Adv Mater, 2014, 26(47), 8046

[31] Li Y, Zhong J, Li J. Rich carbon vacancies facilitated solar light-driven photocatalytic hydrogen generation over $g\text{-}C_3N_4$ treated in H_2 atmosphere. Int J Hydrogen Energy, 2022, 47(94), 39886

[32] Liang Q, Li Z, Huang Z H, et al. Holey graphitic carbon nitride nanosheets with carbon vacancies for highly improved photocatalytic hydrogen production. Adv Funct Mater, 2015, 25(44), 6885

[33] Wang Y, Du P, Pan H, et al. Increasing solar absorption of atomically thin 2D carbon nitride sheets for enhanced visible-light photocatalysis. Adv Mater, 2019, 31(40), 1807540

[34] Hu P, Chen C, Zeng R, et al. Facile synthesis of bimodal porous graphitic carbon nitride nanosheets as efficient photocatalysts for hydrogen evolution. Nano Energy, 2018, 50, 376

[35] Xie Y, Li Y, Huang Z, et al. Two types of cooperative nitrogen vacancies in polymeric carbon nitride for efficient solar-driven H_2O_2 evolution. Appl Catal B, 2020, 265, 118581

[36] Yu H, Shi R, Zhao Y, et al. Alkali-assisted synthesis of nitrogen deficient graphitic carbon nitride with tunable band structures for efficient visible-light-driven hydrogen evolution. Adv Mater, 2017, 29(16), 1605148

[37] Shao Y, Hao X, Lu S, et al. Molten salt-assisted synthesis of nitrogen-vacancy crystalline graphitic carbon nitride with tunable band structures for efficient photocatalytic overall water splitting. Chem Eng J, 2023, 454, 140123

[38] Qin Y, Lu J, Zhao X, et al. Nitrogen defect engineering and π-conjugation structure decorated $g\text{-}C_3N_4$ with highly enhanced visible-light photocatalytic hydrogen evolution and mechanism insight. Chem Eng J, 2021, 425, 131844

[39] Zhao D, Dong C L, Wang B, et al. Synergy of dopants and defects in graphitic carbon nitride with exceptionally modulated band structures for efficient photocatalytic oxygen evolution. Adv Mater, 2019, 31(43), 1903545

[40] Zhang D, Guo Y, Zhao Z. Porous defect-modified graphitic carbon nitride via a facile one-step approach with significantly enhanced photocatalytic hydrogen evolution under visible light irradiation. Appl Catal, B, 2018, 226, 1

[41] Li L, Huang Z, Li Z, et al. Defect-rich porous $g\text{-}C_3N_4$ nanosheets photocatalyst with enhanced photocatalytic activity. J Mater

Sci:Mater Electron, 2021, 32(5), 6465
[42] Jiang Y, Sun Z, Tang C, et al. Enhancement of photocatalytic hydrogen evolution activity of porous oxygen doped g-C_3N_4 with nitrogen defects induced by changing electron transition. Appl Catal, B, 2019, 240, 30
[43] Yu T, Xie T, Zhou W, et al. Fumaric acid assistant band structure tunable nitrogen defective g-C_3N_4 fabrication for enhanced photocatalytic hydrogen evolution. ACS Sustainable Chem Eng, 2021, 9(22), 7529
[44] Ren H, Yang D, Ding F, et al. One-pot fabrication of porous nitrogen-deficient g-C_3N_4 with superior photocatalytic performance. J Photochem Photobiol A, 2020, 400, 112729
[45] Xu C Q, Li K, Zhang W D. Enhancing visible light photocatalytic activity of nitrogen-deficient g-C_3N_4 via thermal polymerization of acetic acid-treated melamine. J Colloid Interface Sci, 2017, 495, 27
[46] Xiao Y, Tian G, Li W, et al. Molecule self-assembly synthesis of porous few-layer carbon nitride for highly efficient photoredox catalysis. J Am Chem Soc, 2019, 141(6), 2508
[47] Dang T T, Nguyen T K A, Bhamu K C, et al. Engineering holey defects on 2D graphitic carbon nitride nanosheets by solvolysis in organic solvents. ACS Catal, 2022, 12(21), 13763
[48] Huo T, Ba G, Deng Q, et al. A dual strategy for synthesizing carbon/defect comodified polymeric carbon nitride porous nanotubes with boosted photocatalytic hydrogen evolution and synchronous contaminant degradation. Appl Catal B, 2021, 287, 119995
[49] Liu G, Shi L, Yao L, et al. In-situ synthesis of defects modified mesoporous g-C_3N_4 with enhanced photocatalytic H_2 evolution performance. Int J Energy Res, 2021, 45(7), 10478
[50] Wang X, Li Q, Gan L, et al. 3D macropore carbon-vacancy g-C_3N_4 constructed using polymethylmethacrylate spheres for enhanced photocatalytic H_2 evolution and CO_2 reduction. J Energy Chem, 2021, 53, 139
[51] Do J-L, Friščić T. Mechanochemistry: A force of synthesis. ACS Cent Sci, 2017, 3(1), 13
[52] Ba G, Huo T, Deng Q, et al. Mechanochemical synthesis of nitrogen-deficient mesopore-rich polymeric carbon nitride with highly enhanced photocatalytic performance. ACS Sustainable Chem Eng, 2020, 8(50), 18606
[53] Huang K, Li C, Yang J, et al. Platinum nanodots modified nitrogen-vacancies g-C_3N_4 Schottky junction for enhancing photocatalytic hydrogen evolution. Appl Surf Sci, 2022, 581, 152298
[54] Liang L, Shi L, Wang F, et al. Synthesis and photo-catalytic activity of porous g-C_3N_4: Promotion effect of nitrogen vacancy in H_2 evolution and pollutant degradation reactions. Int J Hydrogen Energy, 2019, 44(31), 16315
[55] Wu J, Li N, Fang H B, et al. Nitrogen vacancies modified graphitic carbon nitride: Scalable and one-step fabrication with efficient visible-light-driven hydrogen evolution. Chem Eng J, 2019, 358, 20
[56] Sun S P, Wang Y R, Gu S, et al. Effects of vacancies on the electronic structures and photocatalytic properties of g-C_3N_4. Vacuum, 2022, 206
[57] Tahir M, Sherryna A, Khan A A, et al. Defect engineering in graphitic carbon nitride nanotextures for energy efficient solar fuels production: A Review. Energ Fuel, 2022, 36(16), 8948
[58] Li Y, He Z, Liu L, et al. Inside-and-out modification of graphitic carbon nitride (g-C_3N_4) photocatalysts via defect engineering for energy and environmental science. Nano Energy, 2022, 105, 108032
[59] Ma Z, Cui Z, Lv Y, et al. Three-in-One: Opened Charge-transfer channel, positively shifted oxidation potential, and enhanced visible light response of g-C_3N_4 photocatalyst through K and S Co-doping. Int J Hydrogen Energy, 2020, 45(7), 4534
[60] Yang Z, Chu D, Jia G, et al. Significantly narrowed bandgap and enhanced charge separation in porous, nitrogen-vacancy red g-C_3N_4 for visible light photocatalytic H_2 production. Appl Surf Sci, 2020, 504, 144407
[61] Zeng Q, Wang X, Jin M, et al. Nitrogen defects-rich porous graphitic carbon nitride for efficient photocatalytic hydrogen evolution. J Colloid Interf Sci, 2020, 578, 788
[62] Gogoi D, Shah A K, Qureshi M, et al. Silver grafted graphitic-carbon nitride ternary hetero-junction Ag/g-C_3N_4 (Urea)-g-C_3N_4 (Thiourea) with efficient charge transfer for enhanced visible-light photocatalytic green H_2 production. Appl Surf Sci, 2021, 558, 149900
[63] Zhang X, Zhang R, Niu S, et al. Enhanced photo-catalytic performance by effective electron-hole separation for MoS_2 inlaying in g-C_3N_4 hetero-junction. Appl Surf Sci, 2019, 475, 355
[64] Xu Y, Wang M, Liu Y, et al. Efficient charge transfer in Co-doped CeO_2/graphitic carbon nitride with N vacancies heterojunction for photocatalytic hydrogen evolution. J Colloid Interface Sci, 2022, 627, 261
[65] Liao Y, Wang G, Wang J, et al. Nitrogen vacancy induced in situ g-C_3N_4 pn homojunction for boosting visible light-driven hydrogen evolution. J Colloid Interf Sci, 2021, 587, 110
[66] Duan Y, Li X, Lv K, et al. Flower-like g-C_3N_4 assembly from holy nanosheets with nitrogen vacancies for efficient NO abatement. Appl Surf Sci, 2019, 492, 166
[67] Gao B, Dou M, Wang J, et al. Efficient persulfate activation by carbon defects g-C_3N_4 containing electron traps for the removal of antibiotics, resistant bacteria and genes. Chem Eng J, 2021, 426, 131677
[68] Yao Y, Ren G, Li Z, et al. Nitrogen Vacancy-induced deposition of Pd nanoparticles onto g-C_3N_4 with greatly improved photocatalytic activity in H_2 Evolution. Solar RRL, 2021, 5(7), 2100145
[69] Liang L, Shi L, Wang F, et al. g-C_3N_4 nano-fragments as highly efficient hydrogen evolution photocatalysts: Boosting effect of nitrogen vacancy. Appl Catal A-Gen, 2020, 599, 117618
[70] Zhang Y, Huang Z, Dong C L, et al. Synergistic effect of nitrogen vacancy on ultrathin graphitic carbon nitride porous nanosheets for highly efficient photocatalytic H_2 evolution. Chem Eng J, 2022, 431, 134101
[71] Mo Z, Xu H, Chen Z, et al. Self-assembled synthesis of defect-engineered graphitic carbon nitride nanotubes for efficient conversion of solar energy. Appl Catal B, 2018, 225, 154
[72] Bard A J, Fox M A. Artificial photosynthesis: Solar splitting of water to hydrogen and oxygen. Accounts Chem Res, 1995, 28(3), 141
[73] Niu P, Dai J, Zhi X, et al. Photocatalytic overall water splitting by graphitic carbon nitride. Info Mat, 2021, 3(9), 931
[74] Zhang Q, Chen X, Yang Z, et al. Precisely tailoring nitrogen defects in carbon nitride for efficient photocatalytic overall water splitting. ACS Appl Mater Interfaces, 2022, 14(3), 3970
[75] Cao S, Piao L, Chen X. Emerging photocatalysts for hydrogen evolution. Trends Chem, 2020, 2(1), 57
[76] Zhang P, Wu L J, Pan W G, et al. Granular polymeric carbon nitride with carbon vacancies for enhanced photocatalytic hydrogen evolution. Solar RRL, 2021, 5(3), 2000796
[77] Tang H, Xia Z, Chen R, et al. Oxygen doped g-C_3N_4 with nitrogen vacancy for enhanced photocatalytic hydrogen evolution. Chem–Asian J, 2020, 15(21), 3456
[78] Liu Y, Zhang Y, Shi L. One-step synthesis of S-doped and nitrogen-defects co-modified mesoporous g-C_3N_4 with excellent photocatalytic hydrogen production efficiency and degradation ability. Colloids and Surfaces A: Physicochem Eng Aspects, 2022, 641, 128577
[79] Lin Y, Yang Y, Guo W, et al. Preparation of double-vacancy modified carbon nitride to greatly improve the activity of photocata-

lytic hydrogen generation. Appl Surf Sci, 2021, 560, 150029
[80] Cheng L, Chen F Y, Zhu Z Q, et al. Vacancy-modified g-C_3N_4 nanosheets via one-step thermal polymerization of thiosemicarbazide precursor for visible-light-driven photocatalytic activity. Mater Chem Phys, 2022, 275, 125192
[81] Li H, Ning F, Chen X, et al. Effect of carbon and nitrogen double vacancies on the improved photocatalytic hydrogen evolution over porous carbon nitride nanosheets. Catal Sci Technol, 2021, 11(9), 3270
[82] Ma X, Cheng H. Synergy of Nitrogen Vacancies and Intercalation of Carbon Species for Enhancing Sunlight Photocatalytic Hydrogen Production of Carbon Nitride. Appl Catal B, 2022, 314, 121497
[83] Ng B J, Tang J Y, Ow L Y, et al. Nanoscale p–n junction integration via the synergetic hybridization of facet-controlled Cu_2O and defect-modulated g-C_3N_4-x atomic layers for enhanced photocatalytic water splitting. Mater Today Energy, 2022, 29, 101102
[84] Zhu Y, Zhong X, Jia X, et al. Bimetallic Ni–Co nanoparticles confined within nitrogen defective carbon nitride nanotubes for enhanced photocatalytic hydrogen production. Environ Res, 2022, 203, 111844
[85] Li Y, Zhong J, Li J. Reinforced photocatalytic H_2 generation behavior of S-scheme NiO/g-C_3N_4 heterojunction photocatalysts with enriched nitrogen vacancies. Opt Mater, 2023, 135, 113296
[86] Shang Y, Fan H, Chen Y, et al. Synergism between nitrogen vacancies and a unique electrons transfer pathway of Ag modified S-scheme g-C_3N_4/CdS heterojunction for efficient H_2 evolution. J Alloy Compd, 2023, 933, 167620
[87] Luo X, Ma H, Gao J, et al. Nickel-Rich Ni_3N Particles Stimulated by Defective Graphitic Carbon Nitrides for the Effective Oxygen Evolution Reaction. Ind Eng Chem Res, 2022, 61(5), 2081
[88] Yang P, Wang L, Zhuzhang H, et al. Photocarving nitrogen vacancies in a polymeric carbon nitride for metal-free oxygen synthesis. Appl Catal B, 2019, 256, 117794
[89] Yang X, Tian L, Zhao X, et al. Interfacial optimization of g-C_3N_4-based Z-scheme heterojunction toward synergistic enhancement of solar-driven photocatalytic oxygen evolution. Appl Catal B, 2019, 244, 240
[90] Berto T F, Sanwald K E, Byers J P, et al. Enabling overall water splitting on photocatalysts by CO-covered noble metal co-catalysts. J Phys Chem Lett, 2016, 7(21), 4358

Jie Li is currently an Associate Professor in Handan University. She obtained her B.Sc. and M. S. from School of Electrical Engineering, Yanshan University in 2006 and 2009, respectively. His research interests are mainly on control theory and control engineering, nanomaterials and devices for photocatalysis.

Kaige Huang is now an undergraduate student at the University of Chinese Academy of Sciences, and is doing his graduation thesis under the supervision of Professor Zhijie Wang. His current research interest focuses on nanomaterials and nano-devices for photocatalysis.

Yanbin Huang doctor of engineering now is an Associate Professor in Hebei University of Engineering. He got his B.Sc. in 2005 from Hebei Normal University and M.S. in 2008 from Hebei University of Technology. After nine years of teaching and scientific research in Hebei University of Engineering, he received his Ph.D. degree in 2020 from University of Chinese Academy of Sciences. Currently his researches focus on nanomaterials for photocatalysis and energy-related sciences.

Zhijie Wang received his BS degree in 2004 from Zhejiang University and PhD degree in 2009 from the Institute of Semiconductors, Chinese Academy of Sciences. After four years of postdoc research in the University of Wyoming and the University of Michigan, he worked as a senior scientist and a junior group leader at the Ilmenau University of Technology (Germany) in the 3D Nanostructuring Group of Professor Yong Lei since 2013. He is currently a professor in the Institute of Semiconductors, Chinese Academy of Sciences. His research interest includes nanomaterials, nano-devices, energy-related sciences, surface science and photoelectrochemistry.

Shizhong Yue received his PhD. degree from the Institute of Semiconductors, Chinese Academy of Sciences (CAS), in 2018. From 2018 to 2022, he joined the Materials and Science of Engineering, at the National University of Singapore, as a research fellow. In 2022, he moved to the Institute of Semiconductors, CAS as an associate professor. His current research interests focus on perovskite solar cells, thermoelectric materials, surface plasmon polaritons laser, and photocatalysis.